**Table 3.** *O*-Glycans Found in Colon Cancer Cell Lines[a]

| O-glycans observed in LS174T | Molecular ions | O-glycans observed in HCT-15 | Molecular ions |
|---|---|---|---|
| Asialo fraction(peak L-1): 25.6% | | Asialo fraction (Peak H-1):13.8% | |
| Galβ1-3GalNAc-2AA | 504 (+) | GlcNAc-GalNAc-2AA | 545 (+) |
| GlcNAc-GalNAc-2AA | 545 (+) | Fucα1-2-Galβ1-3GalNAc-2AA | 649(+) |
| Galβ1-3(GlcNAcβ1-6)GalNAc-2AA$^{\#A1}$ | 707 (+) | Galβ1-3(GlcNAcβ1-6)GalNAc-2AA$^{\#A1}$ | 707 (+) |
| Galβ1-3(Gal-GlcNAcβ1-6)GalNAc-2AA$^{\#A2}$ | 869 (+) | Galβ1-3(Gal-GlcNAcβ1-6)GalNAc-2AA$^{\#A2}$ | 869 (+) |
| Galβ1-3(Gal-(Fuc-)GlcNAcβ1-6)GalNAc-2AA$^{\#A3}$ | 1014(-) | | |
| Galβ1-3(GlcNAc-Gal-GlcNAcβ1-6)GalNAc-2AA$^{\#A4}$ | 1071(-) | | |
| Galβ1-3(Gal-GlcNAc-Gal-GlcNAcβ1-6)GalNAc-2AA$^{\#A5}$ | 1233(-) | | |
| Galβ1-3(Gal-GlcNAc-Gal-(Fuc-)GlcNAcβ1-6)GalNAc-2AA$^{\#A6}$ | 1379(-) | | |
| Galβ1-3(GlcNAc-Gal-GlcNAc-Gal-GlcNAcβ1-6)GalNAc-2AA$^{\#A7}$ | 1436(-) | | |
| Galβ1-3((Gal-GlcNAc)$_2$-Gal-GlcNAcβ1-6)GalNAc-2AA$^{\#A8}$ | 1598(-) | | |
| Galβ1-3((Gal-GlcNAc)$_2$-Gal-(Fuc-)GlcNAcβ1-6)GalNAc-2AA$^{\#A9}$ | 1744(-) | | |
| Monosialo fraction (Peak L-2): 37.1% | | Monosialo fraction (Peak H-2): 23.8% | |
| Galβ1-3(Gal-GlcNAcβ1-6)GalNAc-2AA + NeuAc$_1$$^{\#MS3}$ | 1159(-) | NeuAcα2-3Galβ1-3GalNAc-2AA$^{\#MS1}$ (Sialyl T antigen) | 795(+) |
| Galβ1-3(Gal-(Fuc-)GlcNAcβ1-6)GalNAc-2AA + NeuAc$_1$$^{\#MS4}$ | 1305(-) | Galβ1-3(GlcNAcβ1-6)GalNAc-2AA+ NeuAc$_1$$^{\#MS2}$ | 997(-) |
| Galβ1-3(Gal-(Fuc-)GlcNAcβ1-6)GalNAc-2AA+ NeuAc$_1$ + SO$_3$ | 1385(-) | Galβ1-3(Gal-GlcNAcβ1-6)GalNAc-2AA + NeuAc$_1$$^{\#MS3}$ | 1159(-) |
| Galβ1-3(Gal-GlcNAc-Gal-(Fuc-)(SO$_3$-)GlcNAcβ1-6)GalNAc-2AA$^{\#MS2}$ | 1459(-) | Galβ1-3(Gal-(Fuc-)GlcNAcβ1-6)GalNAc-2AA + NeuAc$_1$$^{\#MS4}$ | 1305(-) |
| Galβ1-3(Gal-GlcNAc-Gal-GlcNAcβ1-6)GalNAc-2AA + NeuAc$_1$$^{\#MS5}$ | 1524(-) | | |
| Galβ1-3(Gal-(Fuc-)GlcNAc-Gal-(Fuc-)(SO$_3$-)GlcNAcβ1-6) GalNAc-2AA$^{\#L3}$ | 1604(-) | | |
| Galβ1-3(Gal-GlcNAc-Gal-(Fuc-)GlcNAcβ1-6)GalNAc-2AA + NeuAc$_1$$^{\#L6}$ | 1670(-) | | |
| Galβ1-3(Gal-(Fuc-)GlcNAc-Gal-(Fuc-)GlcNAcβ1-6)GalNAc-2AA + NeuAc$_1$$^{\#L7}$ | 1816(-) | | |
| Galβ1-3(Gal-(Fuc-)GlcNAc-Gal-(Fuc-)GlcNAcβ1-6)GalNAc-2AA + NeuAc$_1$ + SO$_3$ | 1896(-) | | |
| Galβ1-3((Gal-GlcNAc)$_2$-Gal-GlcNAcβ1-6)GalNAc-2AA + NeuAc$_1$ + SO$_3$ | 1969(-) | | |
| Galβ1-3((Gal-GlcNAc)$_2$-Gal-(Fuc-)GlcNAcβ1-6)-GalNA-2AA + NeuAc$_1$$^{\#D5}$ | 2035(-) | | |
| Galβ1-3(Gal-GlcNAc-Gal-(Fuc-)GlcNAc-Gal-(Fuc-)GlcNAcβ1-6)GalNAc-2AA + NeuAc$_1$ | 2181(-) | | |
| Disialo fraction (Peak L-3, L-4, L-5): 37.1% | | Disialo fraction (Peak H-3, H-4): 62.4% | |
| NeuAcα2-3Galβ1-3(NeuAcα2-6)GalNAc-2AA$^{\#DS1}$ (Disialyl T antigen) | 1085(-) | NeuAcα2-3Galβ1-3(NeuAcα2-6)GalNAc-2AA$^{\#DS1}$ (Disialyl T antigen) | 1085(-) |
| NeuAc-Galβ1-3(NeuAc-Gal-GlcNAcβ1-6)GalNAc-2AA$^{\#DS2}$ | 1450(-) | Galβ1-3(Gal-GlcNAcβ1-6)GalNAc-2AA + SO$_3$ + NeuAc$_1$$^{\#SA1}$ | 1238(-) |
| NeuAc-Galβ1-3(NeuAc-Gal-(Fuc-)GlcNAcβ1-6)GalNAc-2AA | 1596(-) | NeuAc-Galβ1-3(NeuAc-Gal-GlcNAcβ1-6)GalNAc-2AA$^{\#DS2}$ | 1450(-) |
| NeuAc-Galβ1-3(NeuAc-Gal-GlcNAc-Gal-GlcNAcβ1-6) GalNAc -2AA$^{\#D33}$ | 1815(-) | Galβ1-3(Gal-GlcNAc-Gal-GlcNAcβ1-6)GalNAc-2AA + SO$_3$ + NeuAc$_1$ | 1604(-) |
| NeuAc-Galβ1-3(NeuAc-Gal-GlcNAc-Gal-(SO$_3$-)GlcNAcβ1-6) GalNAc -2AA$^{\#S24}$ | 1895(-) | NeuAc-Galβ1-3(NeuAc-Gal-GlcNAc-Gal-GlcNAcβ1-6) GalNAc -2AA$^{\#D63}$ | 1815(-) |
| NeuAc-Galβ1-3(NeuAc-Gal-GlcNAc-Gal-(Fuc-)GlcNAcβ1-6) GalNAc -2AA$^{\#D24}$ | 1961(-) | NeuAc-Galβ1-3(NeuAc-(Gal-GlcNAc)$_2$-Gal-GlcNAcβ1-6) GalNAc -2AA$^{\#D26}$ | 2180(-) |
| NeuAc-Galβ1-3(NeuAc-Gal-(Fuc-)GlcNAc-Gal-(Fuc-)GlcNAcβ1-6)GalNAc -2AA$^{\#D55}$ | 2107(-) | | |
| Galβ1-3((Gal-GlcNAc)$_2$-Gal-(Fuc-)(SO$_3$-)GlcNAcβ1-6) GalNA -2AA+ NeuAc$_1$$^{\#S45}$ | 2115(-) | | |
| NeuAc-Galβ1-3(NeuAc-(Gal-GlcNAc)$_2$-Gal-GlcNAcβ1-6)GalNAc -2AA$^{\#D56}$ | 2180(-) | | |
| Galβ1-3(Gal-GlcNAc-Gal-(Fuc-)(SO$_3$-)GlcNAc-Gal-(Fuc-) GlcNAcβ1-6)GalNAc -2AA + NeuAc$_1$$^{\#S46}$ | 2260(-) | | |
| NeuAc-Galβ1-3(NeuAc-(Gal-GlcNAc)$_2$-Gal-(Fuc-)GlcNAcβ1-6) GalNAc -2AA$^{\#D57}$ | 2326(-) | | |
| NeuAc-Galβ1-3(NeuAc-Gal-GlcNAc-Gal-(Fuc-)GlcNAc-Gal-(Fuc-)GlcNAcβ1-6)GalNAc -2AA$^{\#D58}$ | 2472(-) | | |
| NeuAc-Galβ1-3(NeuAc-(Gal-GlcNAc)$_2$-Gal-(Fuc-)GlcNAcβ1-6) GalNAc -2AA | 2691(-) | | |
| Degradation product | | Degradation product | |
| (Gal-GlcNAc)$_2$-Gal-2AA$^{\#DF2}$ | 1029(-) | NeuAc-Gal-GlcNAc-Gal-2AA$^{\#DF1}$ | 956(+) |
| Gal-GlcNAc-Gal-(Fuc-)GlcNAc-Gal-2AA$^{\#DF3}$ | 1176(-) | | |
| (Gal-GlcNAc)$_2$-Gal-2AA +Fuc | 1541(-) | | |
| NeuAc-Gal-(Fuc-)GlcNAc-Gal-(Fuc-)(SO$_3$-)GlcNAc-Gal-2AA$^{\#DF4}$ | 1691(-) | | |
| NeuAc-(Gal-GlcNAc)$_2$-Gal-2AA +Fuc | 1758(-) | | |

[a] We showed MS/MS data for the glycan with # marks in Supporting Information. The structures in blue are confirmed according to the analogous consideration on the structures of higher/lower series of *O*-glycans. The structures in red are not assigned in the present study, because we could not observe good $MS^n$ data.

**Table 4.** *O*-Glycans Found in Gastric Cancer Cell Lines[a]

| O-glycans observed in MKN45 | Molecular ions | O-glycans observed in MKN7 | Molecular ions |
|---|---|---|---|
| Asialo fraction(Peak M-1): 5.0% | | Asialo fraction (Peak M7-1):0% | |
| Galβ1-3GalNAc-2AA | 504 (+) | | |
| GlcNAc-GalNAc-2AA | 545 (+) | | |
| Galβ1-3(GlcNAcβ1-6)GalNAc-2AA#A1 | 707 (+) | | |
| Monosialo fraction (Peak M-2, M-3): 21.3% | | Monosialo fraction (Peak M7-3, M7-4): 74.6% | |
| NeuAcα2-6GalNAc-2AA +Na (Sialyl Tn antigen) | 654(+) | NeuAcα2-6GalNAc-2AA + Na (Sialyl Tn antigen) | 654(+) |
| NeuAcα2-3Galβ1-3GalNAc-2AA#MS1 (Sialyl T antigen) | 795(+) | NeuAcα2-3Galβ1-3GalNAc-2AA#MS1 (Sialyl T antigen) | 795(+) |
| Galβ1-3(GlcNAcβ1-6)GalNAc-2AA + $NeuAc_1$#MS2 | 998(+) | Galβ1-3(Gal-GlcNAcβ1-6)GalNAc-2AA + $NeuAc_1$#MS3 | 1159(-) |
| Galβ1-3(Gal-GlcNAcβ1-6)GalNAc-2AA + $NeuAc_1$#MS3 | 1159(-) | Galβ1-3(Gal-(Fuc-)GlcNAcβ1-6)GalNAc-2AA#MS4 | 1305(-) |
| Galβ1-3(Gal-GlcNAc-Gal-GlcNAcβ1-6)GalNAc-2AA + $NeuAc_1$#MS5 | 1524(-) | | |
| Galβ1-3((Gal-GlcNAc)$_2$-Gal-GlcNAcβ1-6)GalNAc -2AA + $NeuAc_1$#MS8 | 1889(-) | | |
| Galβ1-3((Gal-GlcNAc)$_3$-Gal-GlcNAcβ1-6)GalNAc -2AA + $NeuAc_1$#MS10 | 2254(-) | | |
| Galβ1-3((Gal-GlcNAc)$_4$-Gal-GlcNAcβ1-6)GalNAc -2AA + $NeuAc_1$#MS12 | 2619(-) | | |
| Galβ1-3((Gal-GlcNAc)$_5$-Gal-GlcNAcβ1-6)GalNAc -2AA + $NeuAc_1$#MS14 | 2984(-) | | |
| Disialo fractions (Peak M-4, M-6): 61.4% | | Disialo fractions (Peak M7-5): 25.4% | |
| NeuAcα2-3Galβ1-3(NeuAcα2-6)GalNAc-2AA#DS1 (Disialyl T antigen) | 1085(-) | NeuAcα2-3Galβ1-3(NeuAcα2-6)GalNAc-2AA#DS1 (Disialyl T antigen) | 1085(-) |
| NeuAc-Galβ1-3(NeuAc-Gal-GlcNAcβ1-6)GalNAc-2AA#DS2 | 1450(-) | | |
| NeuAc-Galβ1-3(NeuAc-Gal-GlcNAc-Gal-GlcNAcβ1-6)GalNAc- 2AA#DS3 | 1815(-) | | |
| NeuAc-Galβ1-3(NeuAc-(Gal-GlcNAc)$_2$-Gal-GlcNAcβ1-6)GalNAc- 2AA #DS6 | 2180(-) | | |
| NeuAc-Galβ1-3(NeuAc-(Gal-GlcNAc)$_3$-Gal-GlcNAcβ1-6)GalNAc- 2AA #DS9 | 2545(-) | | |
| NeuAc-Galβ1-3(NeuAc-(Gal-GlcNAc)$_4$-Gal-GlcNAcβ1-6)GalNAc- 2AA #DS10 | 2910(-) | | |
| NeuAc-Galβ1-3(NeuAc-(Gal-GlcNAc)$_5$-Gal-GlcNAcβ1-6)GalNAc- 2AA #DS11 | 3275(-) | | |
| Trisialo fraction (Peak M-5): 12.3% | | | |
| NeuAc-Gal-GlcNAc- (NeuAc-Gal-GlcNAc)Galb1-3(NeuAcα2-6)GalNAc-2AA#TS1 | 2106(-) | | |
| NeuAc-Gal-GlcNAc- (NeuAc-Gal-GlcNAc)Galb1-3(NeuAcα2-6)GalNAc-2AA+Gal-GlcNAc#TS2 | 2471(-) | | |
| NeuAc-Gal-GlcNAc- (NeuAc-Gal-GlcNAc)Galb1-3(NeuAcα2-6)GalNAc-2AA+(Gal-GlcNAc)$_2$#TS3 | 2836(-) | | |
| NeuAc-Gal-GlcNAc- (NeuAc-Gal-GlcNAc)Galb1-3(NeuAcα2-6)GalNAc-2AA+(Gal-GlcNAc)$_3$#TS4 | 3201(-) | | |
| NeuAc-Gal-GlcNAc- (NeuAc-Gal-GlcNAc)Galb1-3(NeuAcα2-6)GalNAc-2AA+(Gal-GlcNAc)$_4$#TS5 | 3566(-) | | |
| NeuAc-Gal-GlcNAc- (NeuAc-Gal-GlcNAc)Galb1-3(NeuAcα2-6)GalNAc-2AA+(Gal-GlcNAc)$_5$#TS6 | 3931(-) | | |
| Degradation product | | Degradation product | |
| NeuAcα2-3Gal-2AA | 592(+) | NeuAcα2-3Gal-2AA | 592(+) |
| NeuAc-Gal-GlcNAc-Gal-2AA#DP1 | 957(+) | NeuAc-Gal-GlcNAc-Gal-2AA#DP1 | 956(+) |
| NeuAc-(Gal-GlcNAc)$_2$-Gal-2AA#DP4 | 1321(-) | | |
| NeuAc-(Gal-GlcNAc)$_3$-Gal-2AA#DP5 | 1686(-) | | |
| NeuAc-(Gal-GlcNAc)$_4$-Gal-2AA#DP7 | 2051(-) | | |
| NeuAc-(Gal-GlcNAc)$_5$-Gal-2AA | 2416(-) | | |
| NeuAc-(Gal-GlcNAc)$_6$-Gal-2AA#DP8 | 2781(-) | | |

[a] We showed MS/MS data for the glycan with # marks in Supporting Information. The structures in blue are confirmed according to the analogous consideration on the structures of higher/lower series of *O*-glycans. The structures in red are not assigned in the present study, because we could not observe good $MS^n$ data.

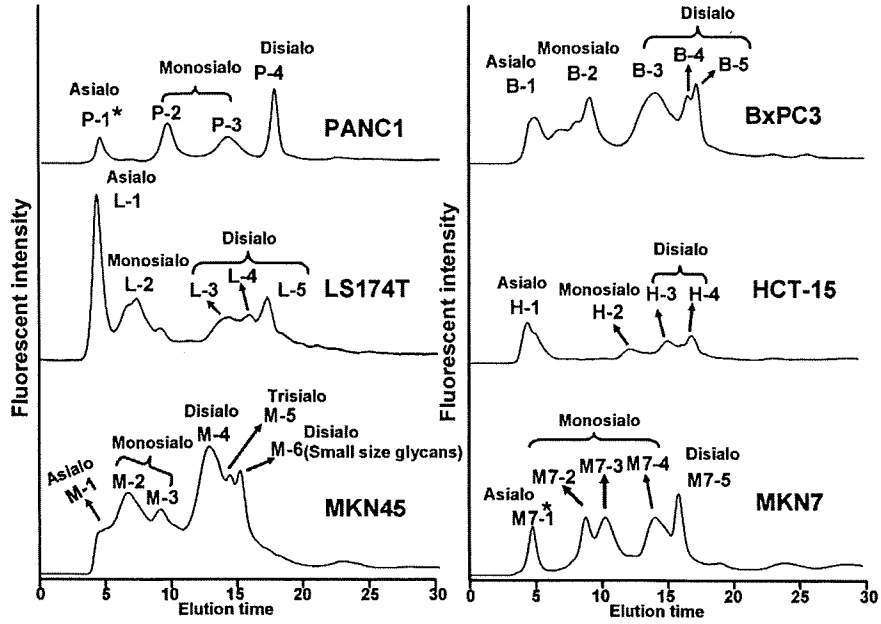


**Figure 4.** Analysis of *O*-glycan pool released from epithelial cancer cells by serotonin-affinity chromatography. Analytical conditions: eluent, solvent A, water; solvent B, 40 mM ammonium acetate; gradient condition, linear gradient (5–75% solvent B) from 2 to 37 min and 75–100% solvent B from 37 to 45 min. The peaks were collected as marked in each chromatogram. The absolute amounts of asiaol-, mono-, di-, trisialo-glycans were determined by the fluorescent intensities of the collected fractions and are summarized in Figure 1.

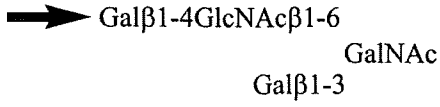


Minor peaks at *m/z* 1961 (#DS4), *m/z* 2326, *m/z* 2691 and *m/z* 3056 due to fucosylated *O*-glycans were also observed among major ions. We analyzed the linkage position of fucose residue. For example, the ion at *m/z* 1961 is considered to have an additional NeuAc residue to the ion at *m/z* 1670 (#MS6) in B-2 fraction. In the $MS^2$ spectra of #MS3, we can see the fragment ion at *m/z* 1014. This means that a Lac*N*Ac residue is released prior to the release of a fucose residue. And based on the similar experimental results as observed in H-12 of HL60 cells, fucose residue is considered to be bound to the most interior Glc*N*Ac residue. Thus, the series of the ions observed at *m/z* 1961 (#DS4), *m/z* 2326 (#DS7), *m/z* 2691 and *m/z* 3056 are due to polylactosamine type *O*-glycans to which a fucose residue attaches to the interior GlcNAc residue. Interestingly, pancreatic tumor tissues highly express Lewis[a] antigens (Galβ1–3(Fucα1–4)Glc*N*Ac-), and most Lewis[a] antigens in BxPC3 cells are located on *O*-glycans as examined by immunoblotting and inhibition studies on biosynthesis of *O*-glycans using benzyl-α-GalNAc.[25] In addition, capillary affinity electrophoresis also showed the presence of *O*-glycans having Lewis[a] structure (data not shown).[24] From the results, fucosylated glycans in peak B-2 and B-3 are assumed to have Lewis[a] structure in their molecules. Disialo-*O*-glycans were also observed in peak B-4 and B-5. Peak B-4 gave two major molecular ion peaks at $[M - H]^-$ = *m/z* 1450 and *m/z* 1815 which correspond to disialo-core2 type glycans, NeuAcα2–3Galβ1–3(NeuAcα2–3Galβ-Glc*N*Acβ1–6)Gal*N*Ac (#DS2) and NeuAcα2–3Galβ1–3(NeuAcα2–3Galβ-Glc*N*Acβ1–3Galβ-Glc*N*Acβ1–6)Gal*N*Ac (#DS3). Peak B5 showed a molecular ion peak at $[M - H]^-$ = *m/z* 1085, which corresponds to disialyl-T antigen (#DS1).

As indicated above, BxPC3 and PANC1 cells showed quite different profiles, although they are from the same organ. Moderately differentiated tumor cell line (i.e., BxPC3) expresses various mucins such as MUC1, MUC2 and MUC5, but poorly differentiated tumor cell lines such as PANC1 express only small amounts of MUC1.[26] At present, we do not have any evidence on the relationship between *O*-glycan profile and cell differentiation, but these differences may be a clue for the guideline of the cancer therapy.

Large amount of asialo *O*-glycans were present in colon cancer cell lines, LS174T and HCT15 cells (Figure 4). Forty-one *O*-glycans in total were identified from LS174T cells by MALDI-TOF MS and most of the *O*-glycans are assumed as the glycans having core2 structures (Figure 6, Table 3).

The asialo fraction (L-1) gave 4 molecular ion peaks as $[M + H]^+$ ions at *m/z* 504, *m/z* 545, *m/z* 707 (#A1) and *m/z* 869 (#A2). Sodium adduct ions at *m/z* 728 and *m/z* 890 were also present. The molecular ion at *m/z* 504 was assigned as core1 structure of Galβ1–3Gal*N*Ac. The molecular ion at *m/z* 707 corresponds to core2 structure. The ion at *m/z* 869 corresponds to galactosyl core2 structure of Galβ1–3(Galβ1–4Glc*N*Acβ1–6)Gal*N*Ac (#A2). In negative ion mode, additional 10 molecular ion peaks were observed as $[M - H]^-$ ions in peak L-1. Four molecular ions at *m/z* 1071 (#A4), *m/z* 1233 (#A5), *m/z* 1436 (#A7) and *m/z* 1598 (#A8) are assigned as core2 structures modified with Hex*N*Ac, $Hex_2Hex$*N*Ac, $Hex_2Hex$*N*$Ac_2$ and $Hex_3Hex$*N*$Ac_2$, respectively, and indicate that these glycans commonly have polylactosamine structures. These polylactosamine-type glycans showed similar fragmentations for the $MS^n$ analysis of polylactosamine glycans of BXPC3 cells. The molecular ion at *m/z* 1014 corresponds to galactosyl core2 structure modified with a fucose residue, and this glycan is considered to have Galβ1–3(Galβ1–4(Fucα1–3)GlcNAcβ1–6)GalNAc, although accurate structural

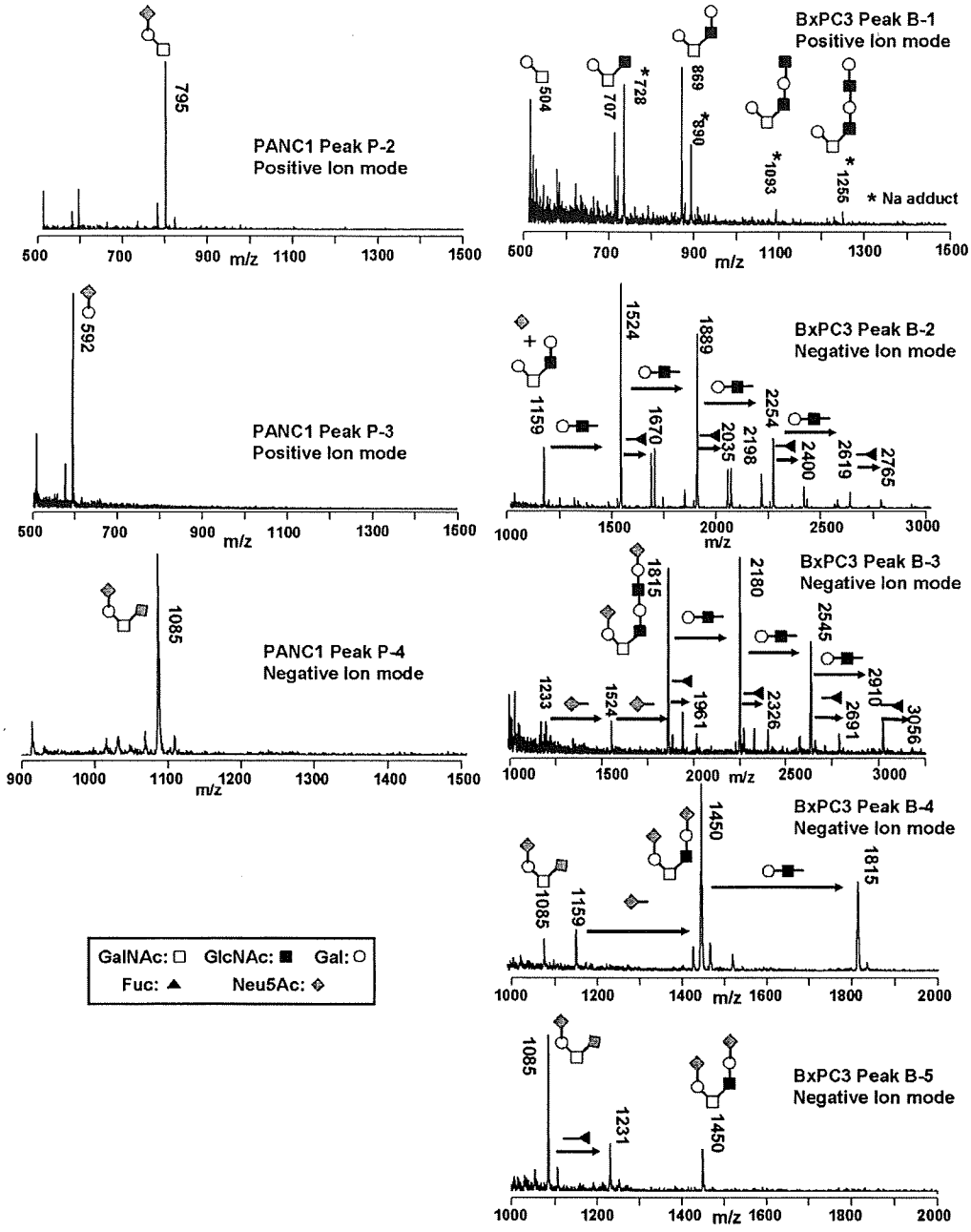


**Figure 5.** MALDI-TOF MS analysis of *O*-glycan fractions derived from PANC1 and BxPC3 cells. The panels in the figure indicate the results on the fractions separated by serotonin affinity chromatography.

confirmation is currently underway. Two molecular ions at *m/z* 1379 (#A6) and *m/z* 1744 (#A9) commonly have core2 structure to which $Hex_2HexNAcdHex$ and $Hex_3HexNAc_2dHex$ are attached, and are considered to have fucosylated polylactosamine-type core2 structures. The monosialo fraction (L-2) showed 12 molecular ion peaks. Some molecular ion peaks are due to mono- or difucosylated polylactosamine-type core2 structures which are modified with an *N*-acetylneuraminic acid residue. In addition, we found two characteristic molecular ion peaks at *m/z* 1385, *m/z* 1459 (#SU2), *m/z* 1604 (#SU3), *m/z* 1896 and *m/z* 1969, which contain a sulfate group. Although these glycans were eluted at the region where monosialo-glycans were observed, these glycans contained no sialic acid but a sulfate group as examined by MALDI-TOF MS. In the $MS^2$ spectra of #SU2, we can observe the ion due to $Hex_1HexNAc_1dHex_1+SO_3$ at *m/z* 590. These data mean that the sulfate group attaches to the fucose-containing lactosamine unit. And we have already shown that the fucose-residue attaches to the lactosamine unit at the innermost part (i.e., reducing side). From these data, we conclude that #SU2 has the following structure.

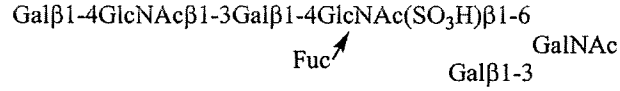


In the similar manner, we also confirmed the structure of the peak observed at *m/z* 1604 as shown in #SU3. *O*-Glycans

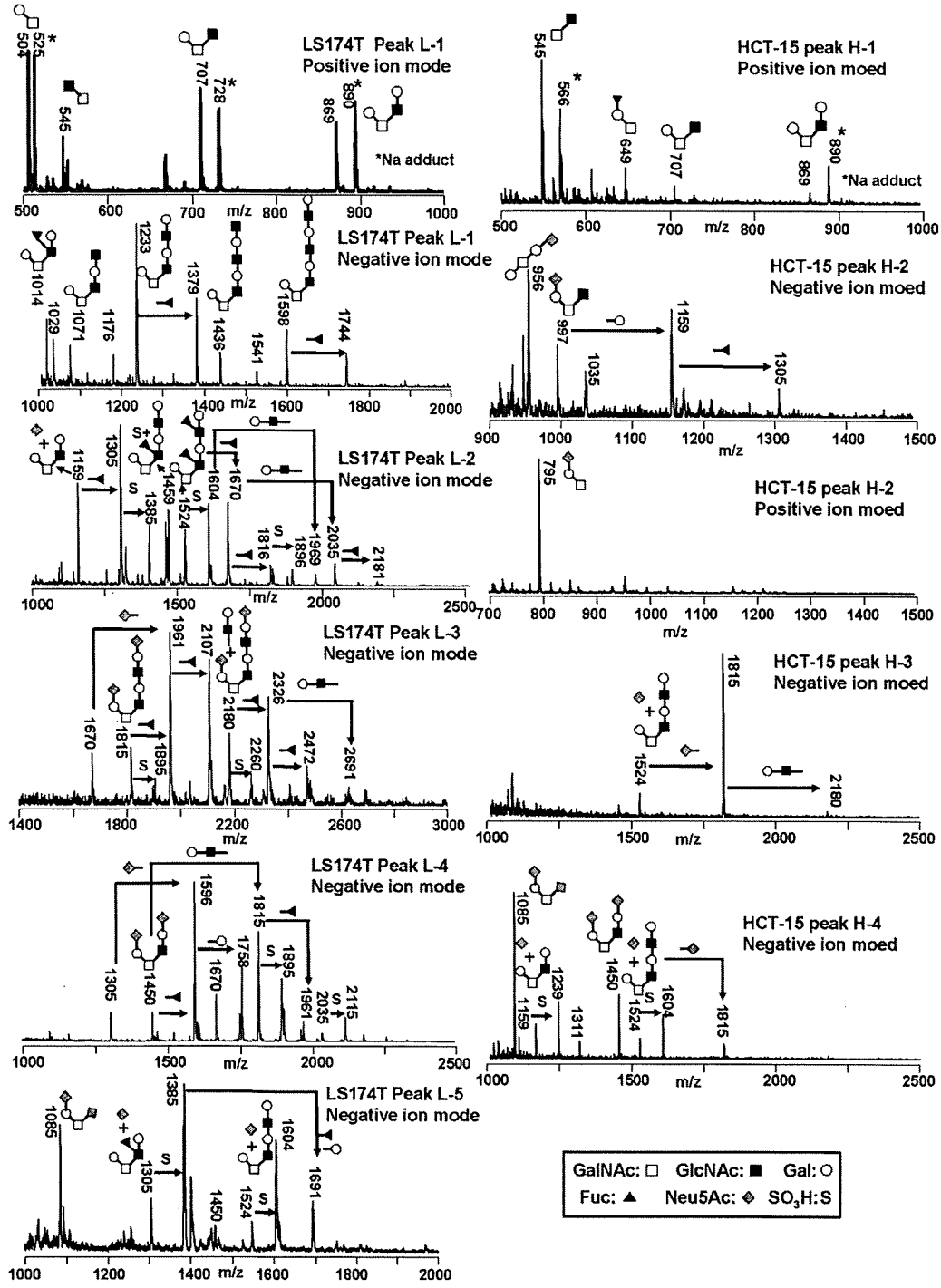


**Figure 6.** MALDI-TOF MS analysis of *O*-glycan fractions derived from LS174T and HCT-15 cells. The panels in the figure indicate the results on the fractions separated by serotonin affinity chromatography.

containing sulfate group(s) are often observed in normal colon tissues. In colon cancer tissues, it was reported that sulfation of *O*-glycans was decreased.[27] However, the loss of sulfation has not been shown in colon cancer tissues in the present study. Similar observation was also reported that *O*-glycans produced by LS174T-HM7, which is a subcell line of LS174T, were modified with sulfate group(s).[28] Disialo-glycan fractions (peak L-3, peak L-4 and peak L-5) showed 15 molecular ions in total. These molecular ions correspond to polylactosamine-type core2 structures which have the similar structural features to those observed in monosialo fractions. Disialo glycans having large molecular masses were observed in L-3, and the biggest one showed the molecular ion at *m/z* 2691 ($NeuAc_2Hex_5HexNAc_5$-$dHex_1$-2AA). The peak is considered to have four lactosamine units and a fucose residue. Two molecular ion peaks at *m/z* 1815 (#DS3) and *m/z* 2180 (#DS6) are $NeuAc_2$ $Hex_3$ $HexNAc_3$ −2AA and $NeuAc_2$ $Hex_4$ $HexNAc_4$ −2AA, and have two and three lactosamine units, respectively. In addition, four molec-

ular ion peaks observed at *m/z* 1961 (#DS4), *m/z* 2107 (#DS5), *m/z*2326 (#DS7) and *m/z* 2472 (#DS8) are due to $NeuAc_2Hex_3HexNAc_3dHex_1$-2AA, and $NeuAc_2Hex_3HexNAc_3dHex_2$-2AA, $NeuAc_2Hex_4HexNAc_4dHex_1$-2AA and $NeuAc_2Hex_4HexNAc_4dHex_2$-2AA, respectively. These glycans contain one or two fucose residues. Other minor ion peaks observed at *m/z* 1895 (#SU4), *m/z* 2115 (#SU5) and *m/z* 2260 (#SU6) are due to sulfated glycans, which correspond to $NeuAc_2Hex_3HexNAc_3SO_3H$-2AA and $NeuAc_2Hex_4HexNAc_4SO_3H$-2AA, respectively. Disialo *O*-glycans of smaller sizes were observed in peak L-4. The molecular ion peak observed at *m/z* 1450 (#DS2) is due to $NeuAc_2Hex_2HexNAc_2$-2AA, which has galactosyl core2 structure (NeuAc-Gal$\beta$1−3(NeuAcGal$\beta$1−4GlcNAc$\beta$1−6)GalNAc). The ions observed at *m/z* 1305 and *m/z* 1670 are due to fragment ions formed by the release of one *N*-acetylneuraminic acid residue. Disialo *O*-glycans having smaller sizes were observed in L-5. The molecular ion peak observed at *m/z* 1085 is due to disialyl-T antigen. Three molecular ions observed at *m/z* 1385, *m/z* 1604 and *m/z* 1691 are due to sulfated glycans, $NeuAc_1Hex_2HexNAc_2dHex_1SO_3H$-2AA, $NeuAc_1Hex_3HexNAc_3SO_3H$-2AA and $NeuAc_2Hex_3HexNAc_2dHex_2SO_3H$-2AA, respectively.

HCT-15 is the same cell line with LS174T (human colorectal adenocarcinoma), but the glycans showed simple profile (Figure 4). The asialoglycan fraction in HCT-15 (H-1) gave four major molecular ions at *m/z* 545, *m/z* 649, *m/z* 707 (#A1) and *m/z* 869 (#A2). The molecular ion at *m/z* 545 is due to $HexNAc_2$-2AA, and corresponds to four possible mucin-type core structures (i.e., core3 structure (GlcNAc$\beta$1−3Gal*N*Ac), core5 structure (Gal*N*Ac$\alpha$1−3Gal*N*Ac), core6 (GlcNAc$\beta$1-6GalNAc) or core7 structure (Gal*N*Ac$\alpha$1−6Gal*N*Ac)). Because the glycans having core 3 structure are often observed in normal colon, the ion at *m/z* 545 is probably due to core 3 type glycan.[29] The molecular ion at *m/z* 649 corresponds to $Hex_1HexNAc_1dHex_1$-2AA, and is assigned as fucosylated core1 type glycan (Fuc$\alpha$1−2Gal$\beta$1−3Gal*N*Ac; H-antigen), which is a typical fucose-containing glycan.[30]

Recently, we reported that significant amount of unusual free sialo glycans derived from complex-type *N*-glycans are specifically accumulated in stomach cancer-derived cell lines, MKN7 and MKN45.[21] Biochemical analyses indicated that these free glycans are cytosolic glycans derived from lysosomes due to the low integrity of lysosomal membrane. In addition, we also reported that *N*-glycans released from cell membrane fractions of MKN45 contain large amount of complex-type *N*-glycans which have multiple fucose residues.[11] On the basis of these observations, we have especially strong interest in *O*-glycan profiles of MKN cells. The results on the *O*-glycan profiles of MKN45 cells are shown in Figure 7 and Table 4.

The asialo fraction (M-1) gave three molecular ions at *m/z* 504, *m/z* 545 and *m/z* 707 (#A1), which correspond to core1, core3 and core2 structures, respectively. Monosialo fractions gave characteristic series of ions at *m/z* 1159 (#MS3), *m/z* 1321 (#DP4), *m/z* 1524 (#MS5), *m/z* 1686 (#DP5), *m/z* 1889 (#MS8), *m/z* 2051 (#DP7), *m/z* 2254 (#MS10), *m/z* 2416, *m/z* 2619 (#MS12), *m/z* 2781 (#DP8) and *m/z* 2984 (#MS14). The ions marked with #DP showed characteristic $MS^n$ spectra, and an example is shown in #DP5. #DP5 showed the molecular ion at *m/z* 1686, and has the composition of $NeuAc_1Hex_4HexNAc_3$-2AA. In the $MS^2$ spectra using the ion at *m/z* 1321 (molecular ion) as the precursor ion, it should be noted that we could not find the ion at *m/z* 341 due to GalNAc-2AA. Instead of this ion, we found the ion at *m/z* 300 due to Hex-2AA. These results indicate that the glycan has hexose (i.e., Gal) at the reducing end. As indicated below, MKN45 cells contained characteristic glycans having biantennary core1 structure. During the releasing reaction of *O*-glycans, elimination reaction occurs at the $\beta$1−3 branch. And the released glycans having a single chain possibly with Gal or Glc*N*Ac residue at the reducing ends are assumed to be formed as indicated in Figure 8.

Monosialo *O*-glycans having small molecular masses (M3) were also observed in positive ion mode. The molecular ion at *m/z* 957 (#DP1: $NeuAc_1Hex_2HexNAc_1$-2AA) is presumably NeuAc-Gal-GlcNAc-Gal-2AA, and this is also due to the product by peeling reaction. Six molecular ions assigned as disialo polylactosamine-type *O*-glycans are observed at *m/z* 1450 (#DS2), *m/z* 1815 (#DS3), *m/z* 2180 (#DS6), *m/z* 2545 (#DS9), *m/z* 2910 (#DS10) and *m/z* 3275 (#DS11) in M-4.

Interestingly, we found trisialo glycans in MKN45 cells. M-5 gave the largest molecular ion at *m/z* 3931 (#TS6) in the present study, and the ion was identified as a polylactosamine-type *O*-glycan having three NeuAc residues ($NeuAc_3Hex_8HexNAc_8$-2AA). In addition, other five major molecular ions at *m/z* 2106 (#TS1), *m/z* 2471 (#TS2), *m/z* 2836 (#TS3), *m/z* 3201 (#TS4) and *m/z* 3566 (#TS5) are also due to trisialo glycans substituted with different numbers of lactosamine residues. The structures of these glycans were confirmed by digestion with neuraminidase (Figure 9).

Digestion of M-5 fraction with neuraminidase resulted in release of three *N*-acetylneuraminic acid residues, and revealed that the fraction contained a series of glycans having extremely large molecular masses, because the glycans having *N*-acetylneuraminic acid residues usually show lower sensitivity than those having no *N*-acetylneuraminic acid residues in MS measurement. The largest one (*m/z* 5248) was composed of 11 lactosamine units. Digestion of the produced glycans with $\beta$-galactosidase caused loss of two galactose residues, although digestion of some glycans did not proceed completely. These results indicate that the polylactosamine glycans have biantennary structures, and two of the *N*-acetylneuraminic acid residues occupy the nonreducing termini and the remaining *N*-acetylneuraminic acid attaches to the interior part of the glycan chain. From the biosynthetic pathway of core structures of *O*-glycans, we conclude that the residual *N*-acetylneuraminic acid probably attaches to the 6-position of Gal*N*Ac residue at the reducing end. From these results, the series of glycans have the following structures:

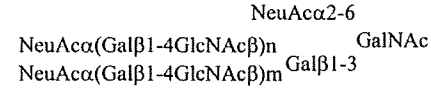


The presence of monosialo-straight chain glycans is another piece of evidence for trisialo-glycans as observed in the analysis of monosialo-glycan fractions such as #DP4−#DP8. However, further biosynthetic studies are necessary to confirm this speculation. At any rate, this is probably the first report that such large polylactosamine glycans having three *N*-acetylneuraminic acid residues are present in human cancer cells. It was reported that MKN45 cells express highly fucosylated N-linked glycans abundantly and polylactosaminyl N-linked glycans are not detected.[11] Polylactosamine-type *N*- and *O*-glycans are synthesized by concerted works of $\beta$1−3-*N*-acetylglucosaminyl transferase and $\beta$1−4galactosyl transferase. But the enzymes involved in the synthesis of *N*- and *O*-glycans are

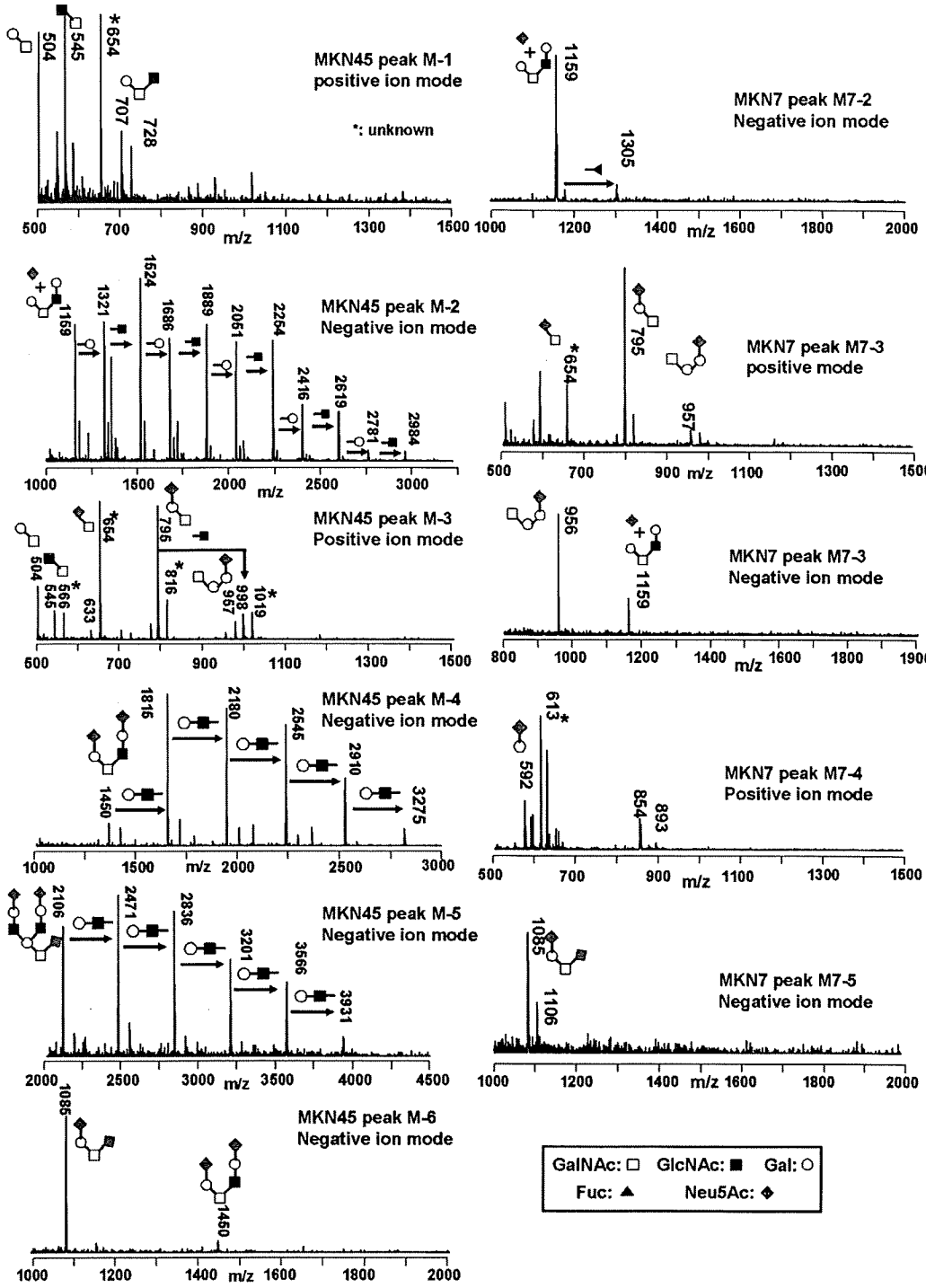


**Figure 7.** MALDI-TOF MS analysis of *O*-glycan fractions derived from MKN45 and MKN7 cells. The panels in the figure indicate the results on the fractions separated by serotonin affinity chromatography.

not the same,[31-33] and the results observed in the present study are the evidence that there are different pathways for modification of nonreducing ends such as with fucosylation and polylactominylation between *N*- and *O*-glycans.

Only six *O*-glycans were observed in MKN7 cells. The early observed peak (neutral glycans, M7−1) did not show MS peaks due to *O*-glycans. Two molecular ions were observed at *m/z* 1159 (#MS3) and *m/z* 1305 (#MS4) in M7−2. These molecular ions were assigned as monosialo galactosyl core2 structures with or without fucose residue. Small monosialo *O*-glycans were observed in M7−3. The molecular ion observed at *m/z* 795 (#MS1) was due to sialyl-T antigen. The molecular ion at *m/z* 654 corresponds to sodium adduct ion of sialyl-Tn antigen. The molecular ion peak at *m/z* 957 corresponds to $NeuAc_1Hex_2HexNAc_1$-2AA (#DP1), which is considered to be a decomposed product during releasing reaction. M7−5 gave a molecular ion

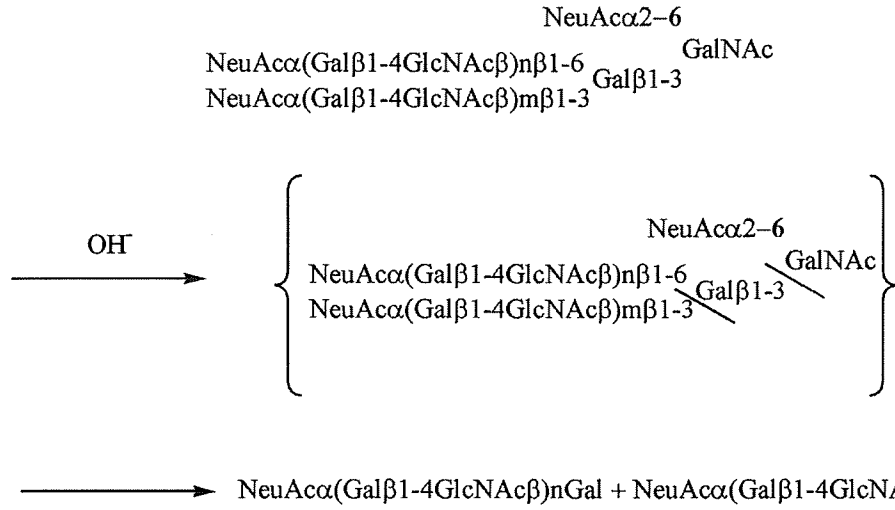


**Figure 8.** Mechanism on the formation of monosialo glycans having single chain from trisialoglycans. The lines in the structure indicate the possible cleavage sites by peeling reaction.

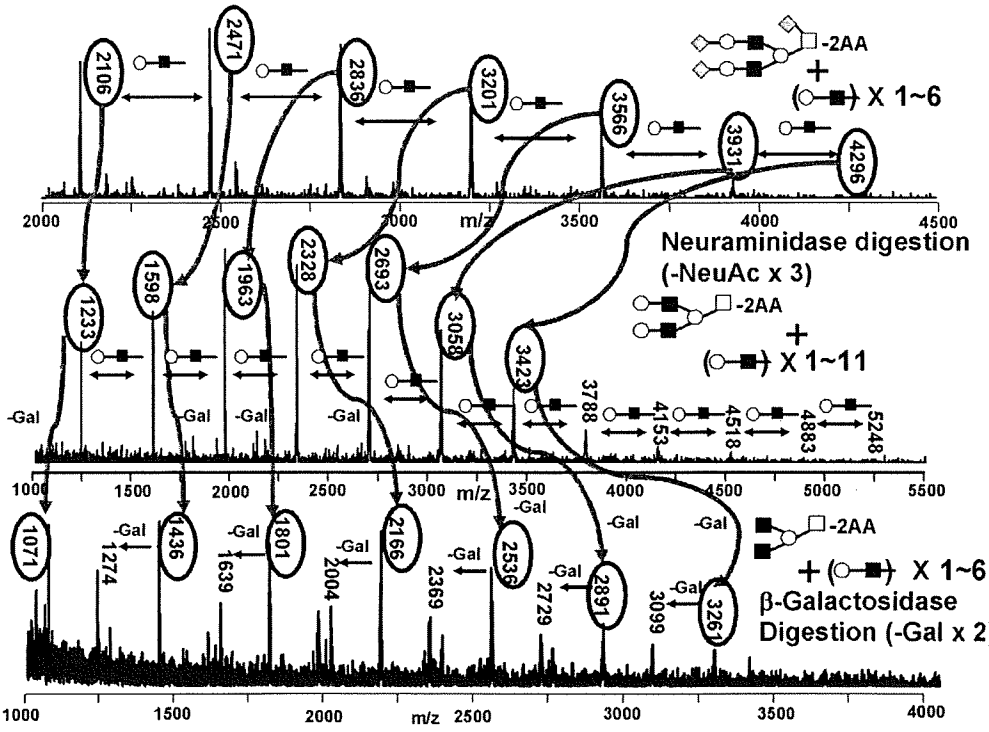


**Figure 9.** Structural analysis of polylactosamine-type *O*-glycans having three *N*-acetylneuraminic acid residues in MKN45 cells. The trisialo-fractions (M-5) in MKN45 cells were collected by serotonin affinity chromatography (see Figure 4), digested with neuraminidase (middle panel), and then with β-galactosidase. Neuraminidase digestion caused loss of three NeuAc residues. Then, digestion with β-galactosidase caused loss of two galactose residues, although some of the asialo-polylactosamine glycans could not be completely released by β-galactosidase.

at *m/z* 1085 (#DS1), and is assigned as disialyl-T antigen. MKN7 cells, well-differentiated tubular adenocarcinoma derived from stomach, and MKN45 cells (poorly differentiated adenocarcinoma also derived from stomach) showed quite different *O*-glycan profiles. MKN7 cells express relatively simple *O*-glycans, and the major glycans are monosialo core2 glycan and sialyl-T antigen. In sharp contrast, MKN45 cells express a large variety of glycans having a number of lactosamine units at Glc*N*Acβ1−3Galβ1−3Gal*N*Ac branch (core1 structure).

## Conclusion

In the present paper, we performed comparative analyses of *O*-glycans in some leukemia and epithelial cells. *O*-Glycans in leukemia cells generally showed simple profiles, and we found that sialyl-T and disialyl-T antigens are the major glycans. This is quite different from *N*-glycan profiles. For example, there are extremely large amount of polylactosamine type *N*-glycans in U937 cells.[11]

PANC1 cells, poorly differentiated epithelial cell line from pancreas, showed only sialyl-T and disialyl-T antigens. However, BxPC3 cells also from pancreas are moderately differentiated tumor cells, and showed relatively complex *O*-glycan profiles. In sharp contrast with these results, MKN45 cells (poorly differentiated species) and MKN7 cells (well-differentiated cells) showed the reverse results, and MKN45 cells showed quite complex *O*-glycan profiles, and large portions of the *O*-glycans were polylactosamine-type glycans. Similar results were also observed in HCT-15 and LS174T cells both from colorectal adenocarcinoma. The *O*-glycan profiles from both cell lines were quite different. It was reported that HCT15 cells were highly tumorigenic, but LS174T cells were poorly proliferative.[22] There is emerging evidence that cell-surface mucins contribute to the regulation of differentiation and proliferation of cancer cells through process of ligand−receptor interactions and morphogenetic signal transduction.[7] Prior to starting this work, we had expected that poorly and well-differentiated cancer cells showed similar tendency of the glycan profiles even from different tissues. The results, however, showed quite different results. Further studies are required to understand these differences, and may give many clues for the new paradigm on biology of cancers.

We noticed that Tn antigen (Gal*N*Ac-*O*-Ser/Thr) was present in some cancer cells. However, the present cleanup method using a Sephadex column for the labeled glycans was not appropriate for collection of small molecules such as GalNAc-2AA (i.e., Tn antigen). We are now establishing a method for quantitative analysis of Tn and sialyl-Tn antigens, and the results will be shown elsewhere.

In the present study, we used the newly developed apparatus for the rapid release of *O*-glycans from the core protein. Although the apparatus can release the *O*-glycans within a few minutes, substantial peeling reaction is observed. We evaluated the rate of the peeling reaction using some model glycoproteins such as fetuin, IgA and porcine stomach mucin.[19] However, we have to continue studies on the effect of peeling reaction on the other heterogeneity repertoire. Luckily, we found series of characteristic trisialo-glycans which have elongated biantennary carbohydrate chains at Gal$\beta$1−3 Glc*N*Ac branch (i.e., core1 structure). In this case, we can identify the peeling product by examining the ion due to Hex-2AA (i.e., Gal-2AA) at $m/z$ 300 in $MS^3$ spectra. Peeling reaction is certainly unfavorable reaction in the analysis of *O*-glycans for quantitative base, but precise $MS^n$ analysis affords valuable information on the determination of *O*-glycan branches.

**Supporting Information Available:** MS analysis of *O*-glycans derived from cancer cells. This material is available free of charge via the Internet at http://pubs.acs.org.

## References

(1) Piller, F.; Piller, V.; Fox, R. I.; Fukuda, M. Human T-lymphocyte activation is associated with changes in O-glycan biosynthesis. *J. Biol. Chem.* **1988**, *263* (29), 15146–15150.

(2) Nakayama, T.; Watanabe, M.; Katsumata, T.; Teramoto, T.; Kitajima, M. Expression of sialyl Lewis(a) as a new prognostic factor for patients with advanced colorectal carcinoma. *Cancer* **1995**, *75* (8), 2051–2056.

(3) Brockhausen, I. Sulfotransferases involved in glycoprotein synthesis. *Biochim. Soc. Trans.* **2003**, *31*, 318–325.

(4) Brockhausen, I. Glycodynamics of mucin biosynthesis in gastrointestinal tumor cells. *Adv. Exp. Med. Biol.* **2003**, *535*, 163–188.

(5) Singhal, A.; Fohn, M.; Hakomori, S. Induction of alpha-N-acetylgalactosamine-O-serine/threonine (Tn) antigen-mediated cellular immune response for active immunotherapy in mice. *Cancer Res.* **1991**, *51* (5), 1406–1411.

(6) Itzkowitz, S. H.; Bloom, E. J.; Kokal, W. A.; Modin, G.; Hakomori, S.; Kim, Y. S. Sialosyl-Tn. A novel mucin antigen associated with prognosis in colorectal cancer patients. *Cancer* **1990**, *66* (9), 1960–1966.

(7) Hollingsworth, M. A.; Swanson, B. J. Mucins in cancer: protection and control of the cell surface. *Nat Rev Cancer* **2004**, *4* (1), 45–60.

(8) Stepensky, D.; Tzehoval, E.; Vadai, E.; Eisenbach, L. O-glycosylated versus non-glycosylated MUC1-derived peptides as potential targets for cytotoxic immunotherapy of carcinoma. *Clin. Exp. Immunol.* **2006**, *143* (1), 139–149.

(9) Takahashi, N. In *Handbook of Endoglycosidases and Glycoamidases*; Takahashi, N.; Muramatsu, T., Eds.; CRC Press: Boca Raton, FL, 1992; p183.

(10) Kamoda, S.; Nakano, M.; Ishikawa, R.; Suzuki, S.; Kakehi, K. Rapid and sensitive screening of N-glycans as 9-fluorenylmethyl derivatives by high-performance liquid chromatography: a method which can recover free oligosaccharides after analysis. *J. Proteome Res.* **2005**, *4* (1), 146–152.

(11) Naka, R.; Kamoda, S.; Ishizuka, A.; Kinoshita, M.; Kakehi, K. Analysis of total N-glycans in cell membrane fractions of cancer cells using a combination of serotonin affinity chromatography and normal phase chromatography. *J. Proteome Res.* **2006**, *5* (1), 88–97.

(12) Kakehi, K.; Susami, A.; Taga, A.; Suzuki, S.; Honda, S. High-performance capillary electrophoresis of O-glycosidically linked sialic acid-containing oligosaccharides in glycoproteins as their alditol derivatives with low-wavelength UV monitoring. *J. Chromatogr., A* **1994**, *680*, 209–215.

(13) Williams, T. I.; Saggese, D. A.; Toups, K. L.; Frahm, J. L.; An, H. J.; Li, B.; Lebrilla, C. B.; Muddiman, D. C. Investigations with O-linked protein glycosylations by matrix-assisted laser desorption/ionization Fourier transform ion cyclotron resonance mass spectrometry. *J. Mass Spectrom.* **2008**, *43* (9), 1215–1223.

(14) Cooke, C. L.; An, H. J.; Kim, J.; Solnick, J. V.; Lebrilla, C. B. Method for profiling mucin oligosaccharides from gastric biopsies of rhesus monkeys with and without Helicobacter pylori infection. *Anal. Chem.* **2007**, *79* (21), 8090–8097.

(15) Zhang, J.; Lindsay, L. L.; Hedrick, J. L.; Lebrilla, C. B. Strategy for profiling and structure elucidation of mucin-type oligosaccharides by mass spectrometry. *Anal. Chem.* **2004**, *76* (20), 5990–6001.

(16) Royle, L.; Mattu, T. S.; Hart, E.; Langridge, J. I.; Merry, A. H.; Murphy, N.; Harvey, D. J.; Dwek, R. A.; Rudd, P. M. An analytical and structural database provides a strategy for sequencing O-glycans from microgram quantities of glycoproteins. *Anal. Biochem.* **2002**, *304* (1), 70–90.

(17) Karlsson, N. G.; Packer, N. H. Analysis of O-linked reducing oligosaccharides released by an in-line flow system. *Anal. Biochem.* **2002**, *305*, 173–185.

(18) Huang, Y.; Mechref, Y.; Novotny, M. V. Microscale nonreductive release of O-linked glycans for subsequent analysis through MALDI mass spectrometry and capillary electrophoresis. *Anal. Chem.* **2001**, *73*, 6063–6069.

(19) Yamada, K.; Hyodo, S.; Matsuno, Y. K.; Kinoshita, M.; Maruyama, S. Z.; Osaka, Y. S.; Casal, E.; Lee, Y. C.; Kakehi, K. Rapid and sensitive analysis of mucin-type glycans using an in-line flow glycan-releasing apparatus. *Anal. Biochem.* **2007**, *371* (1), 52–61.

(20) Matsuno, Y.-k.; Yamada, K.; Tanabe, A.; Kinoshita, M.; Maruyama, S.-z.; Osaka, Y.-s.; Masuko, T.; Kakehi, K. Development of an apparatus for rapid release of oligosaccharides at the glycosaminoglycan-protein linkage region in chondroitin sulfate-type proteoglycans. *Anal. Biochem.* **2007**, *362* (2), 245–257.

(21) Ishiduka, A.; Hashimoto, Y.; Naka, R.; Kinoshita, M.; Kakehi, K.; Seino, J.; Funakoshi, Y.; Suzuki, T.; Kameyama, A.; Narimatsu, H. Accumulation of free complex-type N-glycans in stomach cancer cells, MKN7 and MKN45. *Biochem. J.* **2008**, *413* (2), 227–237.

(22) Trainer, D. L.; Kline, T.; McCabe, F. L.; Faucette, L. F.; Feild, J.; Chaikin, M.; Anzano, M.; Rieman, D.; Hoffstein, S.; Li, D. J.; et al. Biological characterization and oncogene expression in human colorectal carcinoma cell lines. *Int. J. Cancer* **1988**, *41* (2), 287–296.

(23) Maemura, K.; Fukuda, M. Poly-N-acetyllactosaminyl O-glycans attached to leukosialin. The presence of sialyl Le(x) structures in O-glycans. *J. Biol. Chem.* **1992**, *267* (34), 24379–24386.

(24) Nakajima, K.; Oda, Y.; Kinoshita, M.; Kakehi, K. Capillary affinity electrophoresis for the screening of post-translational modification of proteins with carbohydrates. *J. Proteome Res.* **2003**, *2*, 81–88.

(25) Mare, L.; Trinchera, M. Suppression of beta 1,3galactosyltransferase beta 3Gal-T5 in cancer cells reduces sialyl-Lewis a and enhances poly N-acetyllactosamines and sialyl-Lewis x on O-glycans. *Eur. J. Biochem.* **2004**, *271* (1), 186–194.

(26) Sipos, B.; Moser, S.; Kalthoff, H.; Torok, V.; Lohr, M.; Kloppel, G. A comprehensive characterization of pancreatic ductal carcinoma cell lines: towards the establishment of an in vitro research platform. *Virchows Arch.* **2003**, *442* (5), 444–452.
(27) Vavasseur, F.; Dole, K.; Yang, J.; Matta, K. L.; Myerscough, N.; Corfield, A.; Paraskeva, C.; Brockhausen, I. O-glycan biosynthesis in human colorectal adenoma cells during progression to cancer. *Eur. J. Biochem.* **1994**, *222* (2), 415–424.
(28) Capon, C.; Wieruszeski, J. M.; Lemoine, J.; Byrd, J. C.; Leffler, H.; Kim, Y. S. Sulfated lewis X determinants as a major structural motif in glycans from LS174T-HM7 human colon carcinoma mucin. *J. Biol. Chem.* **1997**, *272* (51), 31957–31968.
(29) Yang, J. M.; Byrd, J. C.; Siddiki, B. B.; Chung, Y. S.; Okuno, M.; Sowa, M.; Kim, Y. S.; Matta, K. L.; Brockhausen, I. Alterations of O-glycan biosynthesis in human colon cancer tissues. *Glycobiology* **1994**, *4* (6), 873–884.
(30) Gerken, T. A.; Gilmore, M.; Zhang, J. Determination of the site-specific oligosaccharide distribution of the O-glycans attached to the porcine submaxillary mucin tandem repeat. *J. Biol. Chem.* **2002**, *277*, 7736–7751.
(31) Ujita, M.; McAuliffe, J.; Hindsgaul, O.; Sasaki, K.; Fukuda, M. N.; Fukuda, M. Poly-N-acetyllactosamine synthesis in branched N-glycans is controlled by complemental branch specificity of I-extension enzyme and beta1,4-galactosyltransferase I. *J. Biol. Chem.* **1999**, *274* (24), 16717–16726.
(32) Ujita, M.; McAuliffe, J.; Schwientek, T.; Almeida, R.; Hindsgaul, O.; Clausen, H.; Fukuda, M. Synthesis of poly-N-acetyllactosamine in core 2 branched O-glycans. The requirement of novel beta-1,4-galactosyltransferase IV and beta-1,3-n-acetylglucosaminyltransferase. *J. Biol. Chem.* **1998**, *273* (52), 34843–34849.
(33) Ujita, M.; McAuliffe, J.; Suzuki, M.; Hindsgaul, O.; Clausen, H.; Fukuda, M. N.; Fukuda, M. Regulation of I-branched poly-N-acetyllactosamine synthesis. Concerted actions by I-extension enzyme, I-branching enzyme, and beta1,4-galactosyltransferase I. *J. Biol. Chem.* **1999**, *27414*, 9296–9304.

PR800710F

Analytical Biochemistry 388 (2009) 242–253

Contents lists available at ScienceDirect

Analytical Biochemistry

journal homepage: www.elsevier.com/locate/yabio

# Structural characterization of multibranched oligosaccharides from seal milk by a combination of off-line high-performance liquid chromatography–matrix-assisted laser desorption/ionization–time-of-flight mass spectrometry and sequential exoglycosidase digestion

Mitsuhiro Kinoshita [a], Hiroko Ohta [a], Kanata Higaki [a], Yoko Kojima [a], Tadasu Urashima [b], Kazuki Nakajima [c], Minoru Suzuki [c], Kit M. Kovacs [d], Christian Lydersen [d], Takao Hayakawa [e], Kazuaki Kakehi [a,*]

[a] Faculty of Pharmaceutical Sciences, Kinki University, Kowakae 3-4-1, Higashi-osaka 577-8502, Japan
[b] Graduate School of Food Hygine, Obihiro University of Agriculture and Veterinary Medicine, Obihiro-shi, Hokkaido 080-8555, Japan
[c] Sphingolipid Expression Laboratory; Supra-Biomolecular System Research Group, RIKEN Frontier Research System, Wako-shi, Saitama 351-0198, Japan
[d] Norwegian Polar Institute, N-9007 Tromsø, Norway
[e] Pharmaceutical Research and Technology Institute, Kinki University, Kowakae 3-4-1, Higashi-osaka 577-8502, Japan

ARTICLE INFO

*Article history:*
Received 4 December 2008
Available online 9 March 2009

*Keywords:*
Milk oligosaccharide
Multibranched polylactosamine-type oligosaccharide
MALDI–TOF MS
Exoglycosidase digestion
HPLC

ABSTRACT

A complex mixture of diverse oligosaccharides related to the carbohydrates in glycoconjugates involved in various biological events is found in animal milk/colostrum and has been challenging targets for separation and structural studies. In the current study, we isolated oligosaccharides having high molecular masses (MW ~ 3800) from the milk samples of bearded and hooded seals and analyzed their structures by off-line normal-phase–high-performance liquid chromatography–matrix-assisted laser desorption/ionization–time-of-flight (NP–HPLC–MALDI–TOF) mass spectrometry (MS) by combination with sequential exoglycosidase digestion. Initially, a mixture of oligosaccharides from the seal milk was reductively aminated with 2-aminobenzoic acid and analyzed by a combination of HPLC and MALDI–TOF MS. From MS data, these oligosaccharides contained different numbers of lactosamine units attached to the nonreducing lactose (Galβ1–4Glc) and fucose residue. The isolated oligosaccharides were sequentially digested with exoglycosidases and characterized by MALDI–TOF MS. The data revealed that oligosaccharides from both seal species were composed from lacto-*N*-neohexaose (LNnH, Galβ1–4GlcNAcβ1–6[Galβ1–4GlcNAcβ1–3]Galβ1–4Glc) as the common core structure, and most of them contained Fucα1–2 residues at the nonreducing ends. Furthermore, the oligosaccharides from both samples contained multibranched oligosaccharides having two Galβ1–4GlcNAc (*N*-acetyllactosamine, LacNAc) residues on the Galβ1–4GlcNAcβ1–3 branch or both branches of LNnH. Elongation of the chains was observed at 3-OH positions of Gal residues, but most of the internal Gal residues were also substituted with an *N*-acetyllactosamine at the 6-OH position.



Specific sequences of monosaccharides occur as important structural elements of oligo- and polysaccharides of glycoproteins and glycolipids, and they comprise recognition motifs for ligand–receptor or cell–cell interactions [1–4]. Oligosaccharides are cooperatively synthesized by actions of various glycosyltransferases and are usually present as a complex mixture of diverse oligosaccharides. In particular, the isomeric/branching structure is the major feature, and their structural determination is essential for understanding the biosynthesis and biological significance.

Mammalian milk/colostrum is a rich source of carbohydrates of diverse structures [5–8]. Although the most dominant carbohydrate in mammalian milk is generally lactose, a small amount of characteristic oligosaccharides are also present [9–13]. The milk oligosaccharides usually have a common lactose (Galβ1–4Glc) core that is extended at the 6- and/or 3-OH positions of the Gal as linear/branched mode [14]. Furthermore, the linear/branched chains are frequently fucosylated and/or sialylated and in a few cases are sulfated.

Due to the similarities and complex structures of milk oligosaccharides, structural determination of them has been a big and challenging work. Urashima and coworkers isolated various oligosaccharides from many mammalian species' milk/colostrum and characterized their structural features by a combination of

* Corresponding author. Fax: +81 6 6721 2353.
*E-mail address:* k_kakehi@phar.kindai.ac.jp (K. Kakehi).

0003-2697/$ - see front matter © 2009 Elsevier Inc. All rights reserved.
doi:10.1016/j.ab.2009.03.004

some preparative chromatographic techniques and $^1$H-nuclear magnetic resonance (NMR)[1] spectrometry [14–21]. They reported that milk oligosaccharides contain blood group-related antigens and that their relative abundances are characteristic among animal species. For example, bear milk contains oligosaccharides having an α-Gal epitope (Galα1–3Galβ1–4GlcNAc-R), A blood antigen (GalNAcα1–3[Fucα1–2]Gal-R), B blood antigen (Galα1–3[Fucα1–2]Gal-R), and Lewis$^X$ antigen (Galβ1–4[Fucα1–3]GlcNAc-R) [19]. Urashima and coworkers also reported that milk samples from bearded and hooded seals contain a large amount of neutral oligosaccharides, including lactose (Galβ1–4Glc), 2′-fucosyllactose (Fucα1–2Galβ1–4Glc), and lacto-*N*-fucopentaose (Fucα1–2Galβ1–4GlcNAcβ1–3Galβ1–4Glc) as major components [17,18]. In addition, both milk samples also contain branched oligosaccharides having lacto-*N*-neohexaose (LNnH, Galβ1–4GlcNAcβ1–6[Galβ1–4GlcNAcβ1–3]Galβ1–4Glc) as a core, and most of them have one or two nonreducing α1–2 linked Fuc. Although both milk samples contain sialylated oligosaccharides with high molecular masses, structural studies were not done because of the limited performance of the NMR method. It has also been revealed that milk samples in monotremes such as platypus and echidna contain Lewis$^X$ and Lewis$^Y$ antigens (Fucα1–2Galβ1–4[Fucβ1–3]GlcNAc-R) [10,12,22]. In view of these species-specific structural features and distribution of diverse oligosaccharides in milk/colostrum of different animals, detailed structural studies are not only useful for understanding the underlying evolutionary significance but also promising for using these unique features for biomedical applications.

The dominant carbohydrate in mammalian milk is generally the disaccharide lactose, whereas the milk samples of phocid species, including hooded and bearded seals, contain a variety of oligosaccharides other than lactose [17,18]. The oligosaccharides in bearded and hooded seal milk contain lactose, lacto-*N*-neotetraose (LNnT, Galβ1–4GlcNAcβ1–3Galβ1–4Glc), and LNnH as core units. Furthermore, it is noteworthy that milk oligosaccharides from both species contain type II chain (Galβ1–4GlcNAc-R) but not type I chain (Galβ1–3GlcNAc-R). The presence of α1–3 linked GlcNAc and type II chain suggests that seal mammary glands contain poly-*N*-acetyllactosamines, which are synthesized by β(1–4)galactosyltransferase as well as β(1–3)*N*-acetylglucosaminyltransferase. A search for higher oligosaccharides having poly-*N*-acetyllactosamine structure is an interesting target for understanding the regulation of biosynthesis because they are further modified to form functional oligosaccharides (e.g., sialyl Le$^x$) and/or branched structures.

NMR spectroscopy is the most important technique that provides sequence information including linkage and α/β-anomeric configurations. However, due to the complexity of extremely overlapping signals of the monosaccharide residues in similar environments, especially in the case of oligosaccharides having poly-Galβ1–4GlcNAc (*N*-acetyllactosamine), it is often difficult to assign the branching pattern by only the NMR technique. In contrast, mass spectrometry (MS) has been an indispensable technique for structural analysis of oligosaccharides and useful for the analysis of higher oligosaccharides with high sensitivity. Finke and coworkers reported a method for the analysis of higher oligosaccharides (MW ~ 3000) by a combination of chromatographic separation and matrix-assisted laser desorption/ionization–time-of-flight (MALDI–TOF) MS [23,24]. Recently, tandem mass spectrometry (MS/MS) with collision-induced dissociation (CID) has been applied to structural analysis of various oligosaccharides [25,26]. Chai and coworkers reported a method for the analysis of a complex mixture of isomeric neutral oligosaccharides in human urine and milk samples by nano-liquid chromatography–electrospray ionization–ion trap (LC–ESI–IT) mass spectrometer and identified three novel isomeric fucosylated lacto-*N*-hexaoses (LNHs) based on the studies using CID–MS/MS experiments [27,28]. However, the MS method often cannot differentiate isomeric branched or linear oligosaccharides such as LNnH and *para*-lacto-*N*-hexaose (pLNH, Galβ1–4GlcNAcβ1–3Galβ1–4GlcNAcβ1–3Galβ1–4Glc). Thus, it is still difficult to characterize anomeric configurations, branching configurations, and epimeric forms. This information is often obtained by the analysis of the digestion products with specific exoglycosidases. The molecular mass obtained from MS analysis after digestion with well-defined exoglycosidases reveals the sequence of oligosaccharides and information on the branching pattern.

In this study, we isolated higher oligosaccharides (MW ~ 3800) from bearded and hooded seal milk samples and analyzed their structural characteristics by normal-phase (NP)–HPLC after desialylation with neuraminidase and also by MALDI–TOF MS. Furthermore, we confirmed the branching pattern of the oligosaccharides by a combination of sequential exoglycosidase digestions and MALDI–TOF MS and MALDI–quadrupole ion trap (QIT)–TOF MS.

## Materials and methods

### *Materials*

Milk samples from bearded seal (BS) and hooded seal (HS) were collected from a lactating female in Svalbard, Norway, and from animals on the drifting pack ice in the southern part of the Gulf of St. Lawrence, Canada, respectively. Both milk samples were stored at −20 °C until use. α1–2 Fucosidase derived from *Corynebacterium* sp. and α1–3,4 fucosidase from *Streptomyces* sp. 142 were purchased from Takara Biochemicals (Kusatsu, Japan). α2,3,6,8 Neuraminidase from *Arthrobacter ureafaciens* was kindly donated by Yasuhiro Ohta (Marukin Bio, Kyoto, Japan). β-Galactosidase and β-*N*-acetylhexosaminidase (both from jack beans) were obtained from Seikagaku Kogyo (Tokyo, Japan). All other reagents were analytical or HPLC grade.

### *Fractions containing acidic oligosaccharides from BS and HS milk samples*

Samples of BS and HS milk (40 and 20 ml, respectively) were obtained after delipidation and protein precipitation according to the reported method [17,18]. Briefly, the milk samples were diluted with 4 volumes of distilled water and shaken vigorously with 4 volumes of chloroform/methanol (2:1, v/v). The chloroform layer and denatured protein were discarded. The methanol was removed from the upper layer by a rotary evaporator, and the resulting carbohydrate-containing solution was freeze-dried. Carbohydrate-containing fractions were fractionated on a Biogel P-2 column (2.5 × 100 cm) previously equilibrated with water. An aliquot (0.5 ml) of each fraction was analyzed for hexose by phenol–sulfuric acid assay and for sialic acids by resorcinol assay [29]. Fractions eluted earlier were pooled and lyophilized to dryness (see Fig. 1 in Ref. [17] and Fig. 1 in Ref. [18]). The neutral oligosaccharides of both milk samples and a part of acidic oligosaccharides of bearded seal milk were already characterized in Urashima and coworkers' previous studies [17,18]. The fraction (1.7 mg), which was eluted

[1] *Abbreviations used:* NMR, nuclear magnetic resonance; LNnH, lacto-*N*-neohexaose; LNnT, lacto-*N*-neotetraose; MS, mass spectrometry; MALDI–TOF, matrix-assisted laser desorption/ionization–time-of-flight; MS/MS, tandem mass spectrometry; CID, collision-induced dissociation; LC–ESI–IT, liquid chromatography–electrospray ionization–ion trap; LNH, lacto-*N*-hexaose; pLNH, *para*-lacto-*N*-hexaose; NP, normal-phase; QIT, quadrupole ion trap; BS, bearded seal; HS, hooded seal; 2AA, 2-aminobenzoic acid; DHB, 2,5-dihydroxybenzoic acid; mw, molecular mass; LNnTD, lacto-*N*-neotetradecaose; LNnD, lacto-*N*-neodecaose; LNnDD, lacto-*N*-neododecaose; LNnOD, lacto-*N*-neooctadecaose; GnT, β-*N*-acetylglucosaminyltransferase; iGnT, β3-*N*-acetylglucosaminyltransferase; IGnT, β(1–6)*N*-acetylglucosaminyltransferase.

at void volumes, from the HS milk sample was used in the following preparations and characterization of each oligosaccharide.

The fraction from the BS milk sample was further separated by ion exchange chromatography, as indicated in the previous study [18]. The lyophilized material was dissolved in 50 mM Tris–HCl buffer (pH 8.7, 2.0 ml) and subjected to anion exchange chromatography on a DEAE Sephadex A-50 (1.5 × 35 cm). The unadsorbed oligosaccharide fractions were used for structural study of the oligosaccharides in the previous study [18]. The adsorbed oligosaccharides were eluted by linear gradient elution with changing NaCl concentrations from 0 to 0.25 M in the same buffer. Two fractions (BS1 and BS2) obtained by linear gradient elution were pooled and lyophilized to dryness. The lyophilized material was dissolved in water and passed through a Biogel P-2 column (2.5 × 100 cm). The fractions eluted at the void volume were pooled and lyophilized to dryness to yield a mixture of acidic oligosaccharides (2.0 and 2.3 mg of BS1 and BS2, respectively).

*Fluorescent labeling of oligosaccharides with 2AA*

Fluorescent labeling of oligosaccharides was performed according to the method reported previously [30,31]. Briefly, a solution (250 μl) of 2-aminobenzoic acid (2AA) and $NaBH_3CN$, prepared by dissolution of both reagents (30 mg each) in methanol (1 ml) containing 4% $CH_3COONa$ and 2% boric acid, was added to a mixture of oligosaccharides (100 μg). The mixture was kept at 80 °C for 60 min. After cooling, water (250 μl) was added, and the mixture was applied to a small column (1 × 50 cm) of Sephadex LH-20 previously equilibrated with 50% aqueous methanol. The earlier eluted fluorescent fractions that contained labeled oligosaccharides were collected and evaporated to dryness. The residue was dissolved in water (1 ml), and the solution was stored at −20 °C until analysis.

*Preparation of asialo-oligosaccharides*

A mixture of 2AA-labeled acidic oligosaccharides (~10 μg) was dissolved in 20 mM acetate buffer (pH 5.0, 50 μl), and neuraminidase (10 mU, 10 μl) was added to the mixture. After incubation at 37 °C for 24 h, the reaction mixture was kept in the boiling water bath for 5 min. After centrifugation of the mixture at 10,000g for 10 min, a portion of the supernatant was used for the analysis.

*α-Fucosidase digestion*

A mixture of 2AA-labeled asialo-oligosaccharides (~2 μg), as described above, was dissolved in 20 mM phosphate buffer (pH 7.5, 50 μl) for α1–2 fucosidase digestion or in 20 mM phosphate buffer (pH 6.0, 50 μl) for α1–3,4 fucosidase. α1-2 Fucosidase (40 μU, 2 μl) or α1–3,4 fucosidase (10 μU, 10 μl) was added to the mixture. After incubation at 37 °C for 24 h, the reaction mixture was kept in the boiling water bath for 5 min, and centrifuged at 10,000g for 10 min. The supernatant was diluted with water to adjust the volume of 200 μl. A portion of each solution (5 μl) was used for NP–HPLC analysis.

*Sequential exoglycosidase digestion of oligosaccharides*

Each oligosaccharide isolated by NP–HPLC was dissolved in 20 mM citrate buffer (pH 3.5, 8 μl), and β-galactosidase (1 mU, 2 μl) was added to the mixture. After incubation at 37 °C for 12 h, the reaction mixture was kept in the boiling water bath for 5 min. After centrifugation of the mixture, the supernatant was diluted with water (10 μl). A portion of the solution (2 μl) was analyzed by MALDI–TOF MS. Another portion (5 μl) was mixed with 30 mM citrate buffer (pH 5.0, 5 μl) containing β-*N*-acetylhexosaminidase (5 mU), and the reaction mixture was kept at 37 °C for 12 h. The supernatant was diluted with water (10 μl), and then a portion of the solution (2 μl) was also analyzed by MALDI–TOF MS.

*Separation of the 2AA-labeled oligosaccharides*

HPLC was performed with a Shimadzu apparatus equipped with two LC-6ADvp pumps and an FP-920 fluorescence detector (Waters). Separation was done with an Amide 80 column (TOSOH, 4.6 mm i.d. × 250 mm) using a linear gradient formed by 2% acetic acid in acetonitrile (solvent A) and 5% acetic acid in water containing 3% triethylamine (solvent B). The column was initially equilibrated and eluted with 70% solvent A for 2 min. After 2 min, solvent B was increased to 95% over 80 min and kept for further 20 min [32]. Fluorescence detection was performed at 410 nm by irradiating at 325 nm light.

*MALDI–TOF MS*

MALDI–TOF mass spectra were acquired with a Voyager DE-PRO mass spectrometer (PE Biosystems, Framingham, MA, USA). A nitrogen laser was used to irradiate samples, and an average shot of 50 times was taken. The instrument was operated in a linear mode at an accelerating voltage of 20 kV. An aqueous sample solution (2 μl) was mixed with a matrix solution (2 μl) of 1% 2,5-dihydroxybenzoic acid (DHB) in methanol/water (1:1). The mixture was applied to a polished stainless-steel target and then dried in atmosphere for a few hours.

*MALDI–QIT–TOF MS*

MALDI–QIT–TOF mass spectra were acquired on an AXIMA–QIT–TOF mass spectrometer (Shimadzu, Kyoto, Japan). A nitrogen laser was used to irradiate samples, and an average shot of 50 times was taken. Argon was used for CID. The instrument was operated in positive and reflectron mode. An aqueous sample solution (2 μl) was mixed with a matrix solution (2 μl) of 1% DHB in ethanol/water (1:1), and the mixture was applied to a polished stainless-steel target and dried in atmosphere for a few hours.

## Results

*Acidic oligosaccharides having high molecular masses in BS and HS milk samples*

The method for the preparation of the oligosaccharide samples used in the current study was reported previously [17,18]. Two fractions (BS1 and BS2, 2.0 and 2.3 mg, respectively) from the BS milk sample (40 ml) and a fraction containing acidic oligosaccharides (HS, 1.7 mg) were used in the current study. Because the oligosaccharides from the HS and BS milk samples contained type II chain (Galβ1–4GlcNAc-R) but not type I chain (Galβ1–3GlcNAc-R), we add "neo" to all core oligosaccharide structures.

Oligosaccharides obtained from BS1 and BS2 were fluorescently labeled with 2AA and analyzed by MALDI–TOF MS. As shown in Fig. 1A, a large number of ion signals were observed at the range from *m/z* 1484.8 to *m/z* 3530.4. In BS1, two major molecular ions were observed at *m/z* 2362.3 and 2653.3, which were due to monofucosyl LNnH with one and two NeuAc residues (NAc1H4N2F1–2AA and NAc2H4N2F1–2AA). Ions at *m/z* 2151.0, 3027.9, and 3318.6 are 80 mass units larger than the *m/z* values of monofucosyl LNnH (theoretical molecular mass [mw] 2071.2), difucosyl lacto-*N*-neotetradecaose (LNnTD, theoretical mw 2946.7), and monosialyl difucosyl LNnTD (theoretical mw 3238.6), respectively. These data indicate that these oligosaccharides are substituted with one $SO_3H$ group. In BS2, we observed two major ions at *m/z* 2337.2 and

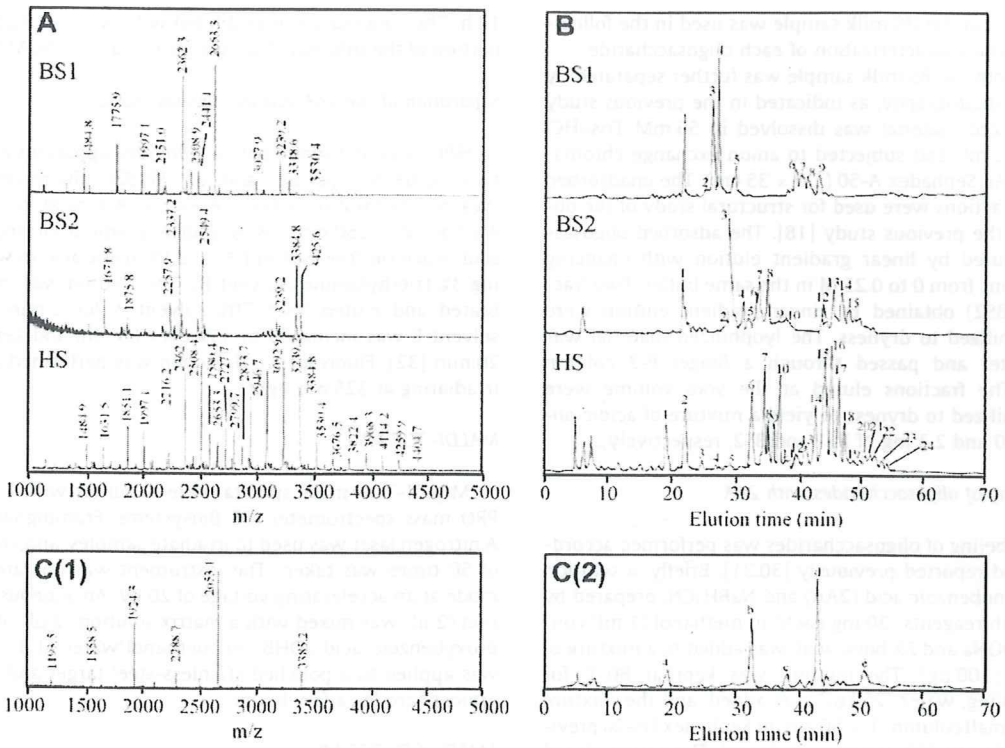


**Fig. 1.** MALDI–TOF MS and NP–HPLC analysis of higher oligosaccharides from bearded and hooded seal milk. (A) MALDI–TOF MS analysis of sialo-oligosaccharides from bearded and hooded seal milk. (B) NP–HPLC analysis of asialo-oligosaccharides from bearded and hooded seal milk. (C) MALDI–TOF MS and NP–HPLC analysis of defucosylated asialo-oligosaccharides from hooded seal milk. BS1, DEAE-adsorbed fraction 1 in BS milk oligosaccharides; BS2, DEAE-adsorbed fraction 2 in BS milk oligosaccharides; HS, higher oligosaccharide fraction in HS milk oligosaccharides; digestion product of HS with α1–2 fucosidase. The monosaccharide compositions of asialo-oligosaccharides are summarized in Table 1.

2549.4, which were due to difucosyl decaose with one $SO_3H$ group (H5N5F2–$SO_3H$–2AA) and monosialo–difucosyl neodecaose with one $SO_3H$ group (NAc1H5N5F2–$SO_3H$–2AA), respectively. The molecular ion observed at *m/z* 3384.8 was due to monosialo LNnTD with three Fuc residues (NAc1H8N6F3–2AA).

HS showed characteristic ladder ions between *m/z* 1400 and *m/z* 4500. These ladder ions were classified into five groups based on the number of lactosamine (Galβ1–4GlcNAc) units. The ions observed at *m/z* 1484.9 and 1631.5 have the composition of NAc1H4N2–2AA and NAc1H4N2F1–2AA, respectively, and are due to mono- and difucosyl LNnH with one NeuAc residue. Molecular ions at *m/z* 1851.1 and 1997.1 are due to the oligosaccharides having compositions of NAc1H5N3–2AA and NAc1H5N3F1–2AA, respectively. A series of the ions at *m/z* 2216.2, 2362.3, 2508.4, and 2653.3 were observed abundantly in HS and are due to the oligosaccharides having monosialo lacto-*N*-neodecaose (LNnD) core (NAc1H6N4–2AA) to which 0, 1, 2, and 3 Fuc residues are attached. Five signals from *m/z* 2946.4 to *m/z* 3530.4 were consistent with oligosaccharides of NAc1H8N6–2AA having 0 to 4 Fuc residues. In addition, we found characteristic glycans having extremely large molecular masses, as observed for the series of ions observed from *m/z* 3676.5 to *m/z* 4404.7. These oligosaccharides are considered to have the core of LNnTD to which 0 to 5 Fuc residues are attached.

To determine linkages of Fuc residues in HS oligosaccharides, we carried out specific fucosidase digestion. A mixture of HS asialo-oligosaccharides was digested with α1–3/4 fucosidase and α1–2 fucosidase, respectively, and the products were analyzed with MALDI–TOF MS. We found that α1–3/4 fucosidase did not act on these oligosaccharides, whereas digestion with α1–2 fucosidase (*Corynebacterium* sp.) caused disappearance of most ions, and six ions were observed at *m/z* 1193.5, 1558.5, 1924.3, 2288.7, 2653.1, and 3385.2 (Fig. 1C(1)). These ions are consistent with the theoretical *m/z* values of H4N2–2AA, H5N3–2AA, H6N4–2AA, H7N5–2AA, H8N6–2AA, and H10N8–2AA, respectively.

The oligosaccharides obtained from milk samples were also analyzed by HPLC using a TSK-Gel Amide-80 column after removing sialic acids with neuraminidase to improve resolution (Fig. 1B) [32]. We collected the major peaks and observed the molecular ions by MALDI–TOF MS. The results are summarized in Table 1.

BS1-1 obtained from the BS1 fraction was assigned as LNnH having two LacNAc units and core Galβ1–4Glc unit from its molecular ion (*m/z* 1193.5) (Fig. 1B, top panel). Molecular ions (*m/z* 2071.8) of BS1-3 and BS1-4 are consistent with the theoretical *m/z* values of H6N4F1–2AA, suggesting the presence of isomers of monofucosyl LNnD. The peak observed at 30 min (BS1-5) gave two molecular ions (*m/z* 2802.6 and 2949.0). The molecular ion at *m/z* 2802.6 is consistent with the theoretical *m/z* value of H8N6F1, suggesting the structure of monofucosyl LNnTD. Likewise, the molecular ion at *m/z* 2949.0 was assigned as difucosyl LNnTD. Minor peaks (BS1-6 to BS1-9) were due to the oligosaccharides having a core structure of LNnD or LNnTD to which a sulfate group is attached (for confirmation of the structure, see the following section).

In the BS2 fraction, BS2-1 and BS2-3 are composed of H3N3F1–2AA and H5N5F2–2AA, respectively. Digestion of BS2-1 and BS2-3 with α1–2 fucosidase caused the loss of one and two fucose residues, respectively. The defucosylated oligosaccharides gave molecular ions corresponding to the theoretical *m/z* values of H3N3–2AA and H5N5–2AA. From the monosaccharide compositions, these oligosaccharides are considered to be hexa- and decasaccharide, having LacNAc units at the reducing end (for confirmation of the structure, see the following section). Oligosaccharides observed be-

**Table 1**
List of asialo-oligosaccharides observed in bearded and hooded seal milk.

| Peak number | Observed mass | Calculated mass | Composition |
|---|---|---|---|
| *(a) BS1* | | | |
| -1 | 1193.5 | 1194.1 | H4N2-2AA |
| -2 | 2110.8 | 2111.9 | H5N5F1-2AA |
| -3 | 2071.8 | 2071.2 | H6N4F1-2AA |
| -4 | 2071.8 | 2071.2 | H6N4F1-2AA |
| -5 | 2802.6 | 2801.7 | H8N6F1-2AA |
| | 2949.0 | 2947.9 | H8N6F2-2AA |
| -6 | 2151.0 | 2151.2 | H6N4F1-$SO_3$H-2AA |
| | 3027.0 | 3027.9 | H8N6F2-$SO_3$H-2AA |
| -7 | 2150.8 | 2151.2 | H6N4F1-$SO_3$H-2AA |
| | 3026.9 | 3027.9 | H8N6F2-$SO_3$H-2AA |
| -8 | 2150.5 | 2151.2 | H8N6F2-$SO_3$H-2AA |
| | 3026.6 | 3027.9 | H6N4F1-$SO_3$H-2AA |
| -9 | 2151.2 | 2151.2 | H6N4F1-$SO_3$H-2AA |
| *(b) BS2* | | | |
| -1 | 1381.6 | 1381.3 | H3N3F1-2AA |
| -2 | 2111.6 | 2111.9 | H5N5F1-2AA |
| -3 | 2259.5 | 2258.2 | H5N5F2-2AA |
| -4 | 2217.7 | 2217.7 | H6N4F2-2AA |
| -5 | 2217.2 | 2217.7 | H6N4F2-2AA |
| | 2363.5 | 2363.7 | H6N4F3-2AA |
| -6 | 2988.7 | 2988.0 | H7N7F2-2AA |
| | 3134.6 | 3134.1 | H7N7F3-2AA |
| -7 | 3134.0 | 3134.1 | H7N7F3-2AA |
| -8 | 2948.7 | 2947.9 | H8N6F2-2AA |
| -9 | 3094.4 | 3093.5 | H8N6F3-2AA |
| -10 | 3240.5 | 3239.2 | H8N6F4-2AA |
| -11 | 2338.1 | 2338.2 | H5N5F2-$SO_3$H-2AA |
| -12 | 2338.2 | 2338.2 | H5N5F2-$SO_3$H-2AA |
| -13 | 2337.8 | 2338.2 | H5N5F2-$SO_3$H-2AA |
| -14 | 2337.5 | 2338.2 | H5N5F2-$SO_3$H-2AA |
| -15 | 3215.5 | 3215.1 | H7N7F3-$SO_3$H-2AA |
| *(c) HS* | | | |
| -1 | 1193.2 | 1194.1 | H4N2-2AA |
| -2 | 1339.3 | 1340.4 | H4N2F1-2AA |
| -3 | 1558.6 | 1559.0 | H5N3-2AA |
| -4 | 1704.9 | 1705.4 | H5N3F1-2AA |
| -5 | 1761.9 | 1762.8 | H5N4-2AA |
| -6 | 1923.9 | 1924.4 | H6N4-2AA |
| -7 | 2068.7 | 2070.0 | H6N4F1-2AA |
| -8 | 2069.5 | 2070.0 | H6N4F1-2AA |
| -9 | 2215.2 | 2216.3 | H6N4F2-2AA |
| -10 | 2215.5 | 2216.3 | H6N4F2-2AA |
| -11 | 2288.8 | 2289.4 | H7N5-2AA |
| | 2363.5 | 2362.3 | H6N4F3-2AA |
| -12 | 2435.6 | 2435.5 | H7N5F1-2AA |
| | 2492.7 | 2492.4 | H7N6-2AA |
| -13 | 2580.9 | 2581.5 | H7N5F2-2AA |
| | 2637.0 | 2638.5 | H7NF1-2AA |
| -14 | 2652.7 | 2654.0 | H8N6-2AA |
| -15 | 2798.6 | 2799.7 | H8N6F1-2AA |
| -16 | 2944.5 | 2945.7 | H8N6F2-2AA |
| -17 | 3089.9 | 3091.7 | H8N6F3-2AA |
| -18 | 3236.4 | 3237.7 | H8N6F4-2AA |
| -19 | 3236.7 | 3237.7 | H8N6F4-2AA |
| -20 | 3382.8 | 3384.1 | H10N8-2AA |
| -21 | 3528.8 | 3530.0 | H10N8F1-2AA |
| -22 | 3674.6 | 3676.3 | H10N8F2-2AA |
| -23 | 3819.8 | 3822.0 | H10N8F3-2AA |
| -24 | 3820.0 | 3822.0 | H10N8F3-2AA |
| *(d) Defucosyl HS* | | | |
| a | 1193.5 | 1194.1 | H4N2-2AA (lacto-*N*-neohexaose) |
| b | 1924.2 | 1924.4 | H6N4-2AA (lacto-*N*-neodecaose) |
| c | 2288.4 | 2289.4 | H7N5-2AA (lacto-*N*-neododecaose) |
| d | 2653.1 | 2654.0 | H8N6-2AA (lacto-*N*-neotetradecaose) |
| e | 3382.5 | 3384.1 | H10HN8-2AA (lacto-*N*-neooctadecaose) |

tween 30 and 38 min (BS2-4 to BS2-10) are considered to have multi-Fuc residues. BS2-4 and BS2-5 have the core structure of the LNnH unit and contain Fucα1–2 residues at the nonreducing ends because these fucose residues were specifically released by digestion with α1–2 fucosidase (data not shown). BS2-6 and BS2-7 showed molecular ions at *m/z* 2988.7 and 3134.6, respectively, which correspond to the compositions of H7N7F2–2AA and H7N7F3–2AA. Peaks BS2-8 to BS2-10 were LNnTD containing multiple Fucα1–2 residues. As a group of characteristic oligosaccharides in BS2, oligosaccharides having 80 mass units larger than BS2-3 were observed between 42 and 49 min. Oligosaccharides (BS2-11 to BS2-14) showed molecular ions at *m/z* 2338.2, indicating the composition of H5N5F2–$SO_3$H–2AA. These oligosaccharides are considered to be isomers having both Fuc and sulfate groups at different positions.

We found 24 oligosaccharide peaks in total in the HS milk sample. These oligosaccharides had LNnH, LNnD, lacto-*N*-neododecaose (LNnDD), LNnTD, and lacto-*N*-neooctadecaose (LNnOD) as core structures (Table 1, part c). HS-1 and HS-2 observed at 20.0 and 21.5 min, respectively, gave molecular ions at *m/z* 1193.2 and 1339.3, which correspond to H4N2–2AA and H4N2F1–2AA, respectively. HS-6, -7, -8, -9, and -10 showed molecular ions at *m/z* 1923.9, 2068.7, 2069.5, 2215.2, and 2215.5, respectively. The molecular ion of HS-6 is consistent with the theoretical mw of H6N4–2AA, suggesting the structure of LNnD. HS-7/8 (*m/z* 2068.7/2069.5) and HS-9/10 (*m/z* 2215.2/2215.5) showed larger molecular ions than those of HS-6 by one Fuc (146 mass units) and two Fuc (292 mass units), respectively. From these results, we concluded that these oligosaccharides had the core structure of LNnD to which different numbers of Fuc residues were attached (for confirmation of the structures, see below). The most abundant group of peaks (HS-14 to HS-19) commonly contains LNnTD (HS-14 at *m/z* 2652.7) as the core structure. HS-15, -16, -17, and -18/19 showed *m/z* values larger than LNnTD by one (146 mass units) to four (584 mass units) Fuc residues. These results indicate that HS-14 to HS-19 have LNnTD unit to which different numbers of Fuc residues are attached. The peaks (HS-20 to HS-24) having high molecular weights (*m/z* 3382.8 to 3820.0) were also observed between 50 and 54 min. These ladder peaks contained LNnOD (theoretical mw 3384.1) as the core structure to which one to four fucose residues are attached.

Urashima and coworkers reported that GlcNAc residues of LNnT and LNnH units in BS and HS oligosaccharides are not fucosylated. In contrast, most GlcNAc residues in bear milk oligosaccharides are fucosylated at OH-3 [17,18]. After digestion of asialo-oligosaccharides derived from HS with α1–3,4 fucosidase from *Streptomyces* sp. 142 or α1–2 fucosidase from *Corynebacterium* sp., the digestion products were analyzed by NP-HPLC. α1–3,4 Fucosidase did not act on the HS oligosaccharides, indicating that the oligosaccharides were not substituted at OH-3/4 on GlcNAc residues with fucose residues (data not shown). In contrast, most peaks disappeared on digestion with α1–2 fucosidase, and five peaks were observed at 19 min (peak a), 32 min (peak b), 38 min (peak c), 43 min (peak d), and 51 min (peak e) (Fig. 1C and Table 1, part d). These data indicated that all core oligosaccharides observed in Fig. 1C(2) were composed of one reducing terminal lactose and 2 to 8 LacNAc units. Peaks a and b showed molecular ions at *m/z* 1193.5 and 1924.2, which correspond to the molecular masses of LNnH and LNnD, respectively. Peak c showed a molecular ion at *m/z* 2288.4 of LNnDD. Peak d was the most abundant one in HS and showed the molecular ion of LNnTD at *m/z* 2653.1. In a similar manner, we confirmed that peak e was due to LNnOD.

### *Characterization of the branching pattern of BS oligosaccharides*

The structures of dominant oligosaccharides in BS1 (BS1-1, -3, and -4 in Fig. 1B) were easily assigned. Digestion of BS1-1 with β-galactosidase from jack beans caused loss of two galactose res-

idues ($\Delta m/z$ 324). Further digestion with β-*N*-acetylhexosaminidase gave a molecular ion at $m/z$ 461 corresponding to lactose with 2AA (data not shown). From the data, we concluded that BS1-1 was substituted with two Gal-GlcNAc residues at Gal OH-6 and Gal OH-3 of lactose. The BS1-3 and BS1-4 were digested with α1–2 fucosidase to afford an ion at $m/z$ 1923.5 corresponding to LNnD. Digestion of the defucosylated oligosaccharide with β-galactosidase caused the loss of three galactose residues ($\Delta m/z$ 486), and the product showed a molecular ion at $m/z$ 1435. From these results, we concluded that the core oligosaccharide of BS1-3 and BS1-4 is substituted with two LacNAc units on either branch of LNnH (data not shown). Oligosaccharides observed between 38 and 42 min gave molecular ions H6N4F1–$SO_3$H–2AA and H8N6F1–$SO_3$H–2AA ($m/z$ 2151.2 and 3026.6, respectively). Among these oligosaccharides, we obtained BS1-9 as nearly pure state (Fig. 2). Digestion of the BS1-9 with α1–2 fucosidase caused the loss of one fucose residue and gave a molecular ion corresponding to LNnD ($m/z$ 2005.1) with a sulfate group. Serial digestions of the defucosylated oligosaccharide with β-galactosidase and β-*N*-acetylhexosaminidase caused the loss of two LacNAc units and gave a molecular ion corresponding to the composition of H4N2–$SO_3$H–2AA ($m/z$ 1275.6). These results indicated that the defucosylated oligosaccharide has two nonsubstituted Gal residues at the nonreducing ends. Further digestion of the oligosaccharide with β-galactosidase gave a molecular ion, H3N2–$SO_3$H–2AA ($m/z$ 1113.3). Urashima and coworkers reported that some oligosaccharides in BS milk were sulfated at the nonreducing terminal Gal OH-3 [18]. From this report and our observations, we concluded that the oligosaccharides from BS1-6 to BS1-9 were due to LNnD and LNnTD substituted with one sulfate group at the OH-3 position of the nonreducing terminal Gal residue.

Structures of dominant oligosaccharides in BS2 (BS2-1 and BS2-3) were confirmed in a similar manner. Digestion of BS2-1 with α1–2 fucosidase caused the loss of one fucose residue (Fig. 3A). Further digestion with β-galactosidase gave a molecular ion ($m/z$ 911.4) corresponding to H3N3–2AA. Finally, digestion with β-*N*-acetylhexosaminidase gave a molecular ion at $m/z$ 505.1 corresponding H1N1–2AA. Accordingly, we concluded that the core disaccharide at the reducing end in BS2-1 was Gal-GlcNAc and that BS2-1 was a hexasaccharide substituted with two LacNAc units at OH-6 and OH-3 of Gal residue of the terminal Gal-GlcNAc. Oligosaccharide BS2–3 was also digested with α1–2 fucosidase to give a glycan showing the molecular ion at $m/z$ 1966.5 corresponding to H5N5–2AA (Fig. 3B). Digestion of the core oligosaccharide with β-galactosidase caused the loss of three galactose residues ($\Delta m/z$ 486). Further digestion with β-*N*-acetylhexosaminidase gave a molecular ion ($m/z$ 869.9) corresponding to H2N2–2AA. Thus, we concluded that one of the branched units on BS2-1 was further substituted with two LacNAc residues. The characteristic oligosaccharides from BS2-11 to BS2-14 showed molecular ions at $m/z$ 2238.1, which are consistent with the composition of H5N5F2–$SO_3$H–2AA. These oligosaccharides were digested with α1–2 fucosidase to produce a signal at $m/z$ 2046.3 corresponding to H5N5–$SO_3$H–2AA. Further digestion of the defucosylated oligosaccharide with β-galactosidase caused the loss of two Gal residues. These observations indicated that the oligosaccharides from BS2-11 to BS2-14 have two LacNAc branches substituted with α1–2 Fuc residue (data not shown).

*Characterization of the branching pattern of HS oligosaccharides*

Digestion of the core oligosaccharide (A, peak a in Fig. 1C(2)) with β-galactosidase caused the loss of two galactose residues

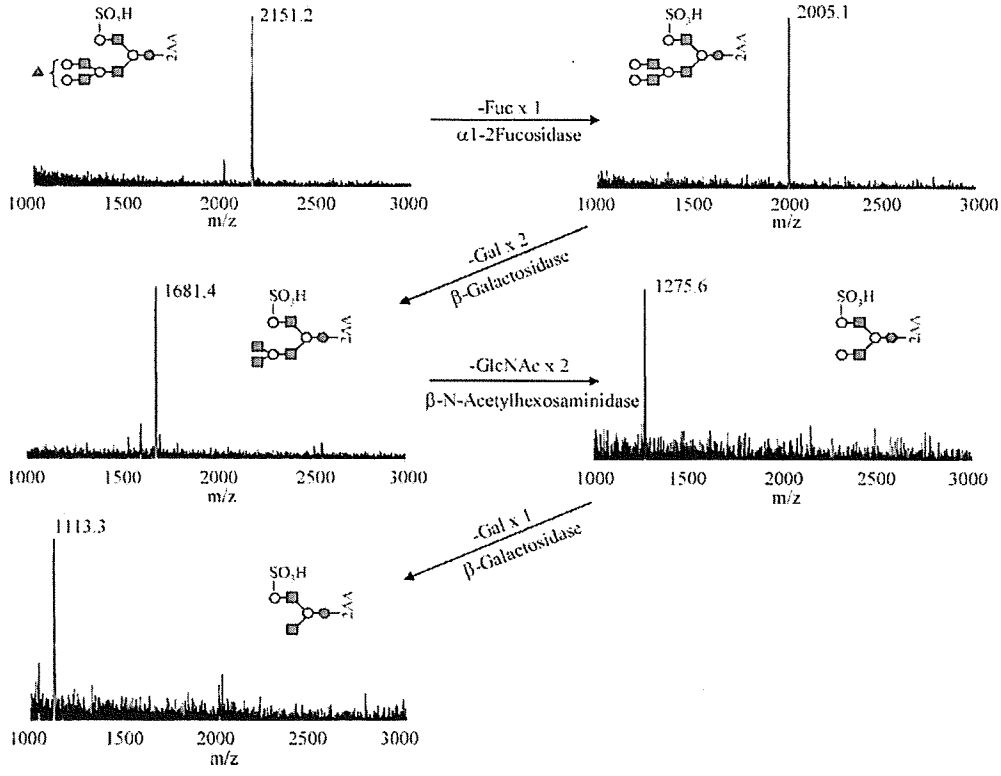


**Fig. 2.** Stepwise exoglycosidase digestion of characteristic oligosaccharide BS1-9 observed in Fig. 1B. Conditions for the enzymatic reaction with exoglycosidases are shown in Materials and methods. Symbols: open circles; Gal; filled circles, Glc; filled squares, GlcNAc; filled triangles, Fuc. Linkage positions are assigned tentatively.

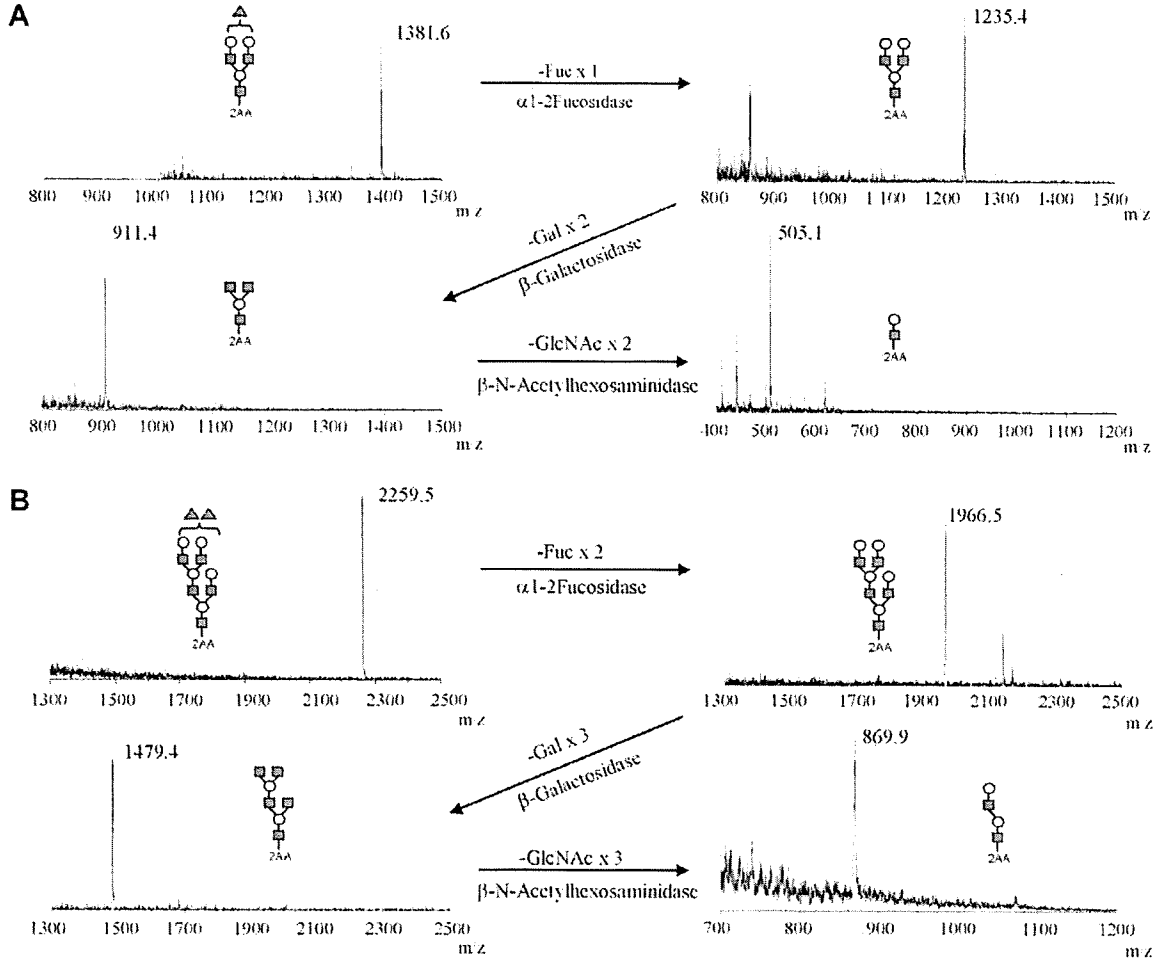


**Fig. 3.** Stepwise exoglycosidase digestion of characteristic oligosaccharides BS2-1 (A) and BS2-3 (B) observed in Fig. 1B. Symbols: open circles, Gal; filled circles, Glc; filled squares, GlcNAc; filled triangles, Fuc. Linkage positions are assigned tentatively.

(Δ*m*/*z* 324) and gave a product ion at *m*/*z* 868.8 (Fig. 4A). The oligosaccharide at *m*/*z* 868.8 was further digested with β-*N*-acetylhexosaminidase, and a new ion corresponding to Gal-Glc-2AA was observed at *m*/*z* 462.4. From these observations, we concluded that the oligosaccharide (peak a) has the structure of Galβ1–4GlcNAcβ1–6[Galβ1–4GlcNAcβ1–3]Galβ1–4Glc (LNnH). Digestion of the core oligosaccharide (B, peak b in Fig. 1C(2)) with β-galactosidase caused the loss of three galactose residues (Δ*m*/*z* 486), and the product showed a molecular ion at *m*/*z* 1437.5 (Fig. 4B). The oligosaccharide at *m*/*z* 1437.5 was further digested with β-*N*-acetylhexosaminidase to release three GlcNAc residues. These observations indicated that the core oligosaccharide (peak b) has a triantennary structure. The produced oligosaccharide corresponding to Gal-GlcNAc-Gal-Glc-2AA (*m*/*z* 826.7) was again digested with β-galactosidase to produce a peak at *m*/*z* 665.1 (GlcNAc-Gal-Glc-2AA). The structure was confirmed by comparison of the retention time with that of trisaccharide (GlcNAcβ1–3Galβ1–4Glc–2AA) prepared by digestion of lacto-*N*-tetraose (Galβ1–3GlcNAcβ1–3Galβ1–4Glc) with β-galactosidase using HPLC on an ODS column and capillary electrophoresis (data not shown). These observations indicated that the core oligosaccharide (peak b) has two LacNAc units on the α1–3 LacNAc branch of LNnH. Digestion of the core oligosaccharide (C, peak c in Fig. 1C(2)) with β-galactosidase caused the loss of three Gal residues (Δ*m*/*z* 486), and the product showed a molecular ion at *m*/*z* 1801.9. The oligosaccharide at *m*/*z* 1801.9 was further digested with β-*N*-acetylhexosaminidase to produce a molecular ion at *m*/*z* 1193.8. The oligosaccharide has the structure of H6N4–2AA. These results indicated that peak c has a triantennary structure. The oligosaccharide (*m*/*z* 1193.8) was again digested with β-galactosidase to produce a peak at *m*/*z* 869.1 by the loss of two galactose residues. The course of digestion by a combination of exoglycosidases revealed that peak c was a dodecasaccharide having three LacNAc residues at nonreducing ends, and we concluded that the oligosaccharide of peak c has two LacNAc units and one LacNAc unit on both branches of LNnH. Digestion of the core oligosaccharide (D, peak d in Fig. 1C(2)) with β-galactosidase caused the loss of four galactose residues (Δ*m*/*z* 648), and the product showed a molecular ion at *m*/*z* 2004.5. The product was further digested with β-*N*-acetylhexosaminidase to produce an ion at *m*/*z* 1193.8 corresponding to LNnH. These observations indicated that peak d has a tetraantennary structure. The produced oligosaccharide corresponding to LNnH was again digested with β-galactosidase to produce a molecular ion at *m*/*z* 869.1. From these results, we concluded that peak d was a tetradecasaccharide having four LacNAc residues at the nonreducing ends and that both branches of LNnH were substituted with two LacNAc units. The oligosaccharide (E, peak e in Fig. 1C(2)) having the largest molecular mass (*m*/*z* 3382.5) present in HS milk caused

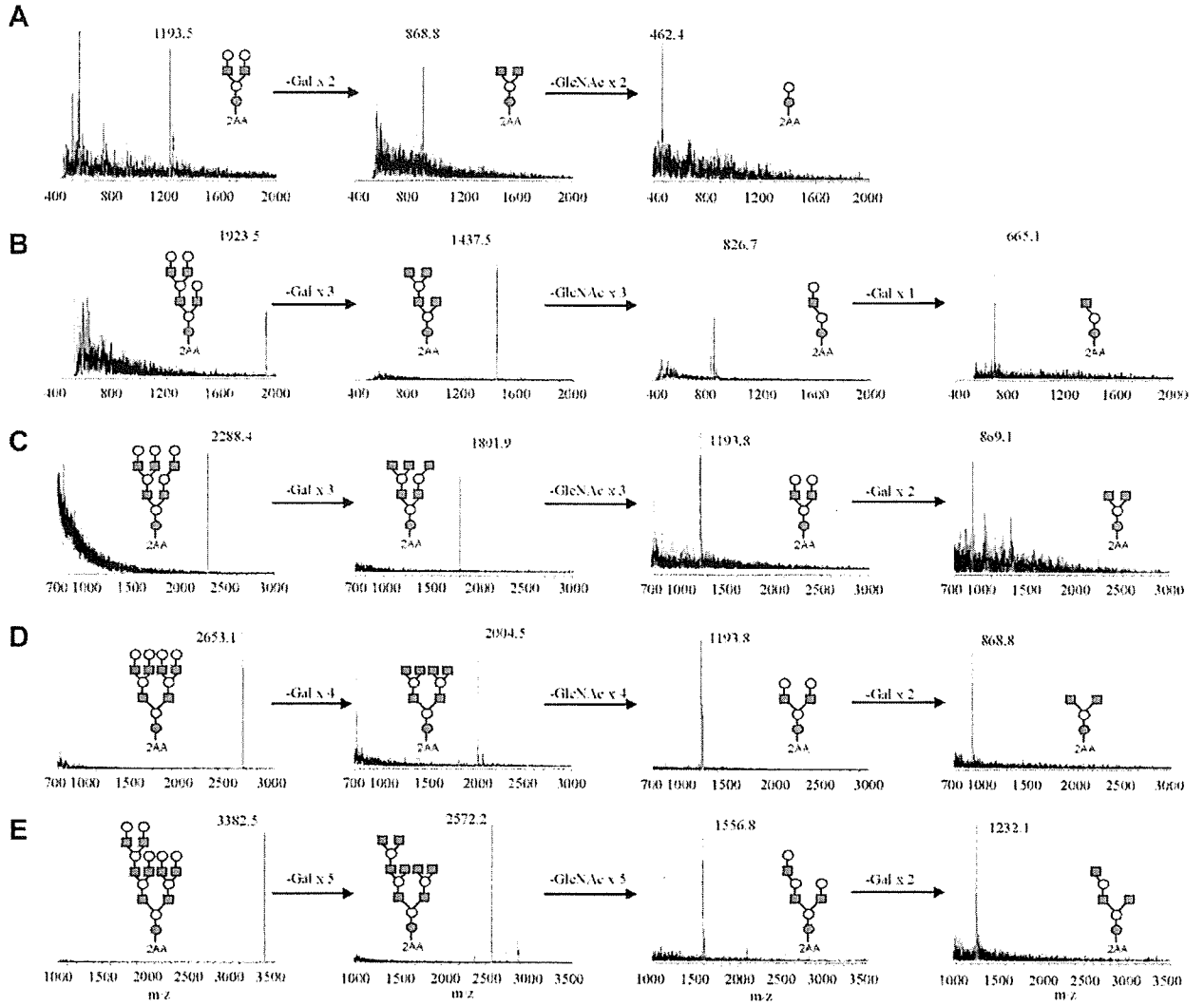


**Fig. 4.** Stepwise exoglycosidase digestion of core oligosaccharides derived from HS observed in Fig. 1B: (A) lacto-*N*-neohexaose (LNnH); (B) lacto-*N*-neodecaose (LNnD); (C) lacto-*N*-neododecaose (LNnDD); (D) lacto-*N*-neotetradecaose (LNnTD); (E) lacto-*N*-neooctadecaose (LNnOD). Symbols: open circles, Gal; filled circles, Glc; filled squares, GlcNAc.

the loss of five galactose residues ($\Delta m/z$ 810) by digestion with β-galactosidase, and the product showed a molecular ion at *m/z* 2572.2. The product was further digested with β-*N*-acetylhexosaminidase to produce a molecular ion at *m/z* 1556.8. The oligosaccharide was again digested with β-galactosidase to produce a peak at *m/z* 1232.1. From these results, we concluded that the oligosaccharide derived from peak e was an octadecasaccharide, as shown in Fig. 4E.

### *Structural determination of fucosylated decasaccharides by MALDI–QIT–TOF MS*

The core oligosaccharides in HS milk are substituted with a different number of fucose residues, as shown by characteristic ladder patterns (Fig. 1B). We purified monofucosylated LNnD (MFLNnD, HS-7, and HS-8 in Fig. 1B) and difucosylated LNnD (DFLNnD, HS-9, and HS-10 in Fig. 1B) and analyzed them using MALDI–QIT–TOF MS. Fig. 5 shows the MS/MS spectra using $[M + Na]^+$ observed at *m/z* 2093.1 for the purified MFLNnD (Fig. 5A and B). The Y ion at *m/z* 1947.5/1947.2 corresponding to the loss of 146 mass units (dHex-18 mass) from $[M + Na]^+$ indicates the presence of a Fuc residue. The Y ions at *m/z* 1728.0/1728.1 and 1581.9/1582.0 are due to H5N3F1–2AA and H5N3–2AA, respectively. These fragment ions were commonly observed in HS-7 and HS-8. We also found the set of B ion series, $[H2N2]^+$ at *m/z* 753.5/754.5, $[H3N3]^+$ at *m/z* 1118.7/1118.8, $[H3N3F1]^+$ at *m/z* 1264.8/1264.9, and $[H4N3F1]^+$ at *m/z* 1791. Characteristic ions observed at *m/z* 1264.8 (Fig. 5A) and *m/z* 1118.8 (Fig. 5B) suggested the difference in the linkage positions of Fuc residues at the nonreducing Gal residues. The B ion at *m/z* 1264.8 ($B_{5\alpha}$) indicates that a Fuc residue is linked to the most outer LacNAc residue. The B ion at *m/z* 1118.8 corresponding to three LacNAc units suggests that one Fuc is attached to the 6-branch side of the reducing terminal lactose. Urashima and coworkers reported that small oligosaccharides in HS milk contained type II LacNAc (Galβ1–4GlcNAc-R) but not type I LacNAc (Galβ1–3GlcNAc-R) [14]. Thus, the oligosaccharides HS-7 and HS-8 are assigned to those as indicated in Fig. 5.

Fig. 6 shows the MS/MS spectra of the ions at *m/z* 2239.8 for the $[M + Na]^+$ of DFLNnD (HS-9 and HS-10 in Fig. 1B). The Y ions at *m/z* 2093.3 corresponding to a loss of 146 (dHex-18 mass) from $[M + Na]^+$ indicate the presence of Fuc residue. In a similar manner, in the case of MS/MS of MFLNnD (Fig. 5), the Y ions observed at *m/z*

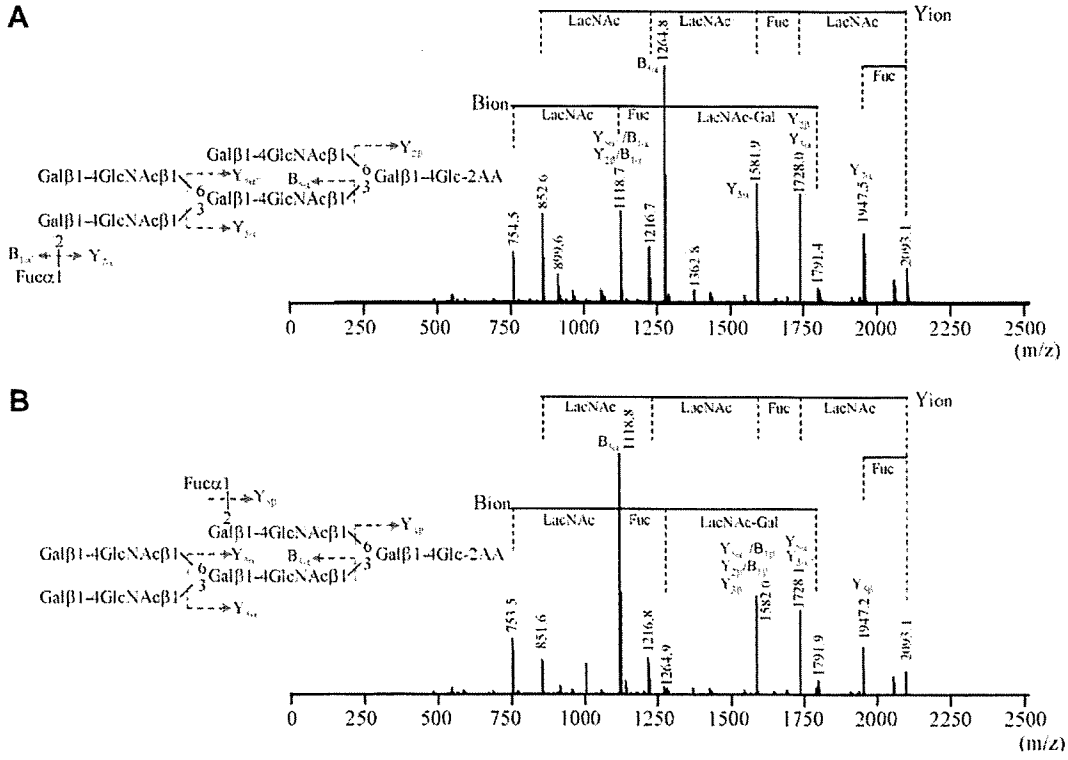


**Fig. 5.** MS/MS spectra of monofucosyl LNnD HS-7 (A) and HS-8 (B). The dotted lines on the spectra indicate type of cleavage (Y or B ion) according to Domon and Costello's nomenclature [48].

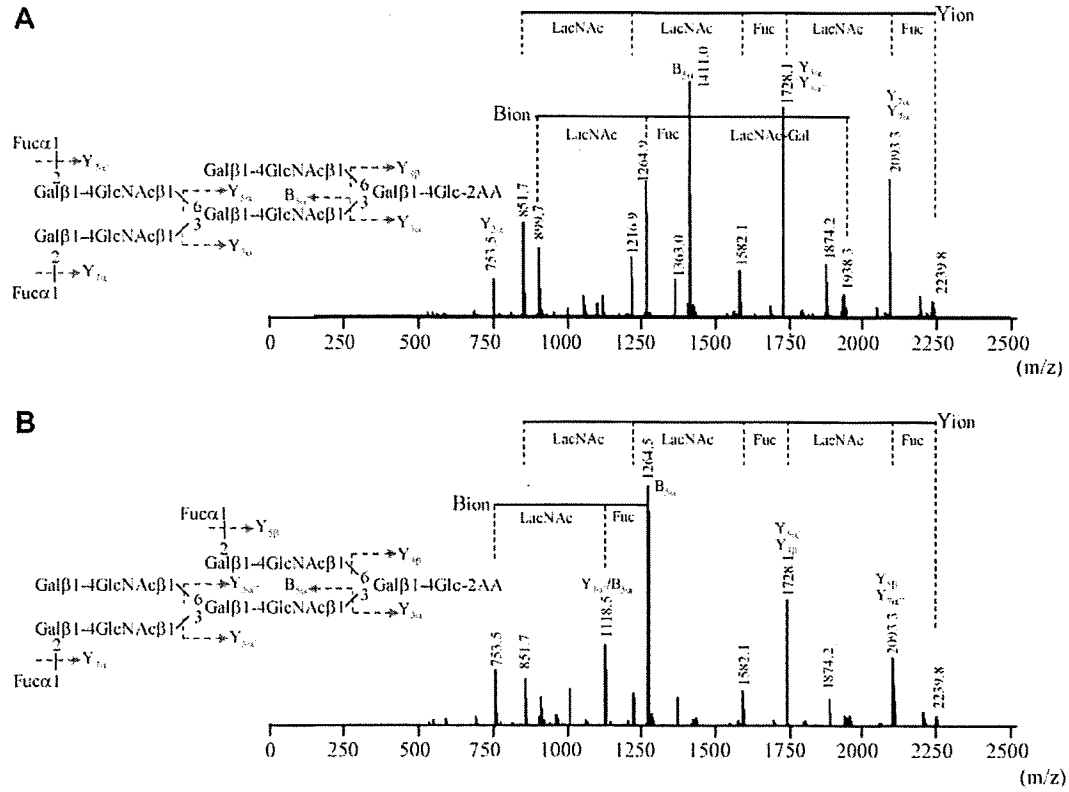


**Fig. 6.** MS/MS spectra of difucosyl LNnD HS-9 (A) and HS-10 (B). The dotted lines on the spectra indicate type of cleavage (Y or B ion) according to Domon and Costello's nomenclature [48].

1728.1 and 1582.1 correspond to [H5N3F1–2AA] and [H5N3–2AA], respectively. The Y ion at *m/z* 851.7 corresponds to the composition of $[H3N1–2AA]^+$. These fragment ions of the Y ion series were commonly observed in HS-9 and HS-10. We also observed the set of B ion series, $[H2N2]^+$ at *m/z* 753.5, $[H2N2F1]^+$ at *m/z* 1118.5, $[H3N3F1]^+$ at *m/z* 1264.5, and $[H3N3F2]^+$ at *m/z* 1411.0. A characteristic ion at *m/z* 1411.0 observed in HS-9 (Fig. 6A), which corresponds to three LacNAc units having two Fuc residues, indicates that two Fuc residues are attached to the nonreducing Gal residues of both LacNAc branches linked to Galβ1–4GlcNAcβ1–3Galβ1–4Glc, as shown in Fig. 6A. Thus, the structure of HS-9 is assigned as shown in Fig. 6A. In contrast, a characteristic ion at *m/z* 1264.5 ($B_{5\alpha}$) observed in HS-10 (Fig. 6B) indicates the attachment of only one Fuc to the most outer LacNAc residue. Therefore, the oligosaccharide (HS-10) is assigned to the structure as shown in Fig. 6B.

Among LNnD substituted with α1–2 Fuc residues, HS-7 and HS-10 were abundantly present (Fig. 1B) and both oligosaccharides have an α1–2 Fuc residue on either LacNAc on the α1–3 branch of the LNnH core. These observations suggest that the modification of multibranched core oligosaccharides with α1–2 Fuc residues proceeds preferably at LacNAc residues of the elongated branches.

## Discussion

We studied structural features of oligosaccharides from the milk samples of bearded and hooded seals by NP–HPLC and MALDI–TOF MS. The combination of sequential digestion of the oligosaccharides with exoglycosidases and MALDI–TOF MS was a useful technique for elucidation of the branching patterns and modification of oligosaccharides with fucose and/or sulfate group(s). Table 2 shows a list of asialo-oligosaccharides found in bearded and hooded seal milk. The oligosaccharides are categorized into nine core structures (A–I) based on the monosaccharide compositions. LNnD and LNnTD (C and E in Table 2) were observed as common core structures in both milk samples, but the two species showed quite different features. The most characteristic fea-

**Table 2**
Structural features of the oligosaccharides derived from bearded and hooded seal milk.

| ID | Core structure | Number of Fuc residues | | | | | ID | Core structure | Number of Fuc residues | | | | |
|---|---|---|---|---|---|---|---|---|---|---|---|---|---|
| | | 0 | 1 | 2 | 3 | 4 | | | 0 | 1 | 2 | 3 | 4 |
| A | 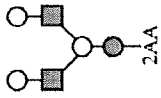 | HS | HS | – | – | – | F | 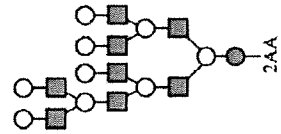 | HS | HS | HS | HS | HS |
| B | 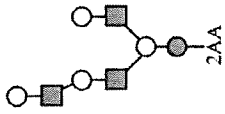 | HS | HS | – | – | – | G | 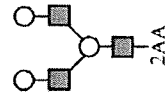 | – | BS | – | – | – |
| C | 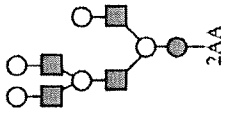 | HS | HS<br>BS | HS<br>BS | HS<br>BS | – | H | 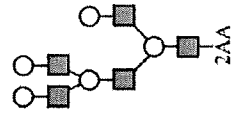 | – | BS | BS | – | – |
| Cs | 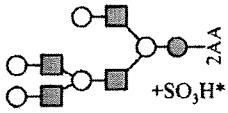 | – | BS | – | – | – | Hs | 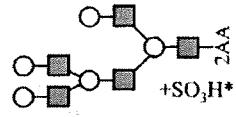 | – | – | BS | – | – |
| D | 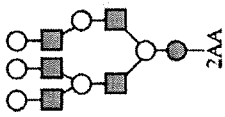 | HS | HS | HS | – | – | I | 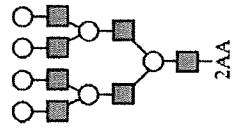 | – | – | BS | BS | – |
| E | 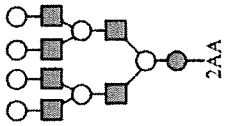 | HS | HS<br>BS | HS<br>BS | HS<br>BS | HS<br>BS | Is | 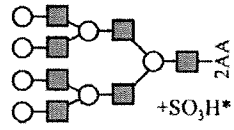 | – | – | – | BS | – |
| Es | 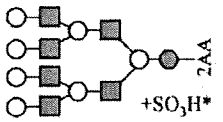 | – | – | BS | – | – | | | | | | | |

*Core structures with sulfate group at 3-OH position of nonreducing terminal Gal.